INFORMATION TO USERS

This reproduction was made from a copy of a document sent to us for microfilming. While the most advanced technology has been used to photograph and reproduce this document, the quality of the reproduction is heavily dependent upon the quality of the material submitted.

The following explanation of techniques is provided to help clarify markings or notations which may appear on this reproduction.

1. The sign or "target" for pages apparently lacking from the document photographed is "Missing Page(s)". If it was possible to obtain the missing page(s) or section, they are spliced into the film along with adjacent pages. This may have necessitated cutting through an image and duplicating adjacent pages to assure complete continuity.

2. When an image on the film is obliterated with a round black mark, it is an indication of either blurred copy because of movement during exposure, duplicate copy, or copyrighted materials that should not have been filmed. For blurred pages, a good image of the page can be found in the adjacent frame. If copyrighted materials were deleted, a target note will appear listing the pages in the adjacent frame.

3. When a map, drawing or chart, etc., is part of the material being photographed, a definite method of "sectioning" the material has been followed. It is customary to begin filming at the upper left hand corner of a large sheet and to continue from left to right in equal sections with small overlaps. If necessary, sectioning is continued again—beginning below the first row and continuing on until complete.

4. For illustrations that cannot be satisfactorily reproduced by xerographic means, photographic prints can be purchased at additional cost and inserted into your xerographic copy. These prints are available upon request from the Dissertations Customer Services Department.

5. Some pages in any document may have indistinct print. In all cases the best available copy has been filmed.

University
Microfilms
International
300 N. Zeeb Road
Ann Arbor, MI 48106

Owolabi, Olubunmi Oyeleye

RESERVOIR FLUID PROPERTIES OF ALASKAN CRUDES

University of Alaska M.S. 1984

RESERVOIR FLUID PROPERTIES OF ALASKAN CRUDES

A

THESIS

Presented to the Faculty of the University of Alaska in Partial Fulfillment of the Requirements for the Degree of

MASTER of SCIENCE

By

Olubunmi Oyeleye Owolabi, B. S.

Fairbanks, Alaska

May 1984

RESERVOIR FLUID PROPERTIES OF ALASKAN CRUDES

RECOMMENDED:

Chairman, Advisory Committee

Department Head

APPROVED:

Director of Graduate Programs

10 May 1984

Date

ABSTRACT

Reservoir fluid properties such as bubble point pressure, solution gas-oil ratio, formation volume factor, and viscosity are essential for the evaluation of reservoir performance. In the absence of laboratory measured pressure-volume-temperature (PVT) data, these properties must be predicted from correlations. Various PVT correlation have been published over the years and empirical relationships among the reservoir fluid properties are available. Alaskan crude oils are distinguished by high non-hydrocarbon contents, which render predictions from the presently used correlations innaccurate without applying some correction factors. This paper presents a series of PVT correlations developed for Cook-Inlet Basin (CIB) and Alaskan North Slope (ANS) crude oils, using laboratory PVT reports collected from operators of Alaskan oil fields.

These new correlations are presented in form of equations as well as nomographs or as graphs. Significant improvement in the predictions of reservoir fluid properties were obtained with the use of the new correlations.

The effect of non-hydrocarbon content on the reservoir fluid properties was also examined.

TABLE OF CONTENTS

TABLE OF CONTENTS

LIST OF FIGURES

LIST OF FIGURES

LIST OF TABLES

ACKNOWLEDGEMENTS

In every human society, no individual is absolutely self-reliant or self-sufficient, and no versatile academician has attained the highest peak of knowledge without the help of others. The successful completion of this program has been the result of various assistances from many people. It should be noted that though few selected individuals have been named here, I wish to state that I am highly indebted to all the people who gave me some helpful suggestions.

I wish to express my appreciation to the authorities and staff of the University of Alaska, most especially the employees and academic staff of the Department of Petroleum Engineering for their friendliness, cooperation and for creating an atmosphere conductive for effective studies.

I thank Dr. Russell D. Ostermann for contributing his knowledge and efforts in directing the thesis. Thanks to Dr. Christine A. Ehlig-Economides and Dr. Michael J. Economides, for their encouragement which was a source of motivation for this study. My sincere thanks to Joyce Cochran and Debbie LaBarre for putting my final manuscripts together.

I wish to thank the technical personnel and the management of ARCO Alaska, Inc. , Shell Oil Company, Union Oil Company of California, and Marathon Oil Company for providing assistance and permission to use data from confidential PVT reports, on which the study is based.

I wish to acknowledge the Alaskan Council of Science and Technology for the financial support which made this study possible.

Finally, special gratitude is expressed to my family for their encouragement and assistance throughout my academic endeavor.

CHAPTER I

INTRODUCTION

Pressure-volume-temperature (PVT) analysis data for petroleum reservoir fluids is used routinely by practicing petroleum engineers to predict petroleum reserves, predict size of reservoir, evaluate strength of water drive and to predict future performance of a pool. The PVT data is also required to design enhanced oil and gas recovery schemes, wellbore flow systems, flow lines, separation and other fluid handling systems.

The oil industry has in the past relied on reservoir fluid physical properties data obtained by laboratory measurements conducted on the bottom-hole sample or proper recombinations of surface trap samples. The need has always arisen to have a fairly accurate correlations of reservoir fluid properties because in the absence of laboratory tests, these properties must be predicted for field measurements. Usually, these properties are required at a time when the only reservoir data available consists of the stock-tank oil gravity, gas gravity, reservoir temperature and the reservoir pressure. To assist in making predictions, various correlations have been presented in the literatures since the early 1940's. Among the major properties of interest are the bubble-point pressure, the formation volume factor at the bubble-point pressure, the solution gas-oil ratio and the oil viscosity.

Of the PVT correlations currently in use, Standings[19] work probably enjoys the widest popularity. However, more recent correlations developed by Lasater[13], Glaso[8], and Vazquez and Beggs[21] are also in common use. The correlation of Vazquez and Beggs[21] form the basis for the PVT correlations used in the Petroleum Fluids Pac for the Hewlett-Packard 41-CV calculator.

Previous PVT correlations have been based on data from limited geographical locations, as in the case of Standing's[19] use of California crudes, or on large composite data bases from a wide variety of areas including crudes of widely differing properties (Vazquez and Beggs[21]). The reservoir fluids behavior is also a strong function of composition. The direct application of correlations which do not take compositional effects into account should be undertaken with caution. If a crude has a particularly unusual composition, neither of the above correlating approaches is likely to be very accurate. The properties of crudes which most influence reservoir fluid property behavior but which are not taken into account in most correlations are paraffinicity and non-hydrocarbon content (N_2, CO_2, and H_2S). Neglecting to apply correction factors for the non-hydrocarbon gases, can result in errors of 30% or more in the prediction of bubble-point pressure.

For the above reasons, the purpose of this present study was to develope some improved correlations that would be most perfect for Alaskan oil fields. The data used for

the development of the correlations were obtained from the flash separation conditions of the laboratory measured PVT analyses, from fields in the Cook Inlet Basin and the Alaskan North Slope.

CHARACTERISTICS OF ALASKAN CRUDES:

There are presently two major petroleum producing provinces in the State of Alaska, the Cook Inlet Basin (CIB), and the Alaskan North Slope (ANS). The ANS is the largest producing field in North American continent, with an estimated recoverable reserves of 9.4 billion barrels of crude oil and condensate, for the Prudhoe Bay Field. The CIB is smaller but a significant region with recoverable reserves of over 3 billion barrels. A brief summary of the oil and gas fields in Alaska is given in Table 1. Also see Figures 1 to 3 for the locations of Prudhoe Bay and Cook Inlet Basin oil and gas fields.

Two distinct genetic oil types predominate across the ANS; the Simpson-Umiat type and the Barrow-Prudhoe type[14]. The first, the Simpson-Umiat oil type, occurs in reservoir rocks of Cretaceous and Quaternary age and includes oil from Cape Simpson and Umiat oil fields. These are higher gravity (37°API), low-sulfur crude oils. There is presently no commercial production of this type of oil. The second type, the Barrow-Prudhoe oil type, occurs in reservoir rocks of Carboniferous to Cretaceous ages and includes crude oils

from south Barrow gas field, and Prudhoe Bay oil field. Physical properties of Barrow-Prudhoe oils are variable, but in general the oils are medium-gravity (27°API), high sulphur crude oils.

Crude oils from the producing oil pools at Prudhoe Bay have high nitrogen and carbon dioxide contents. The high nitrogen content causes the bubble point to be considerably higher than that predicted by the currently available published correlations.

Production in the CIB has primarily been from Tertiary formations. That much of it is from depths of 10,000 feet or more is unusual for Tertiary formations. The first well that produced commercial quantities of oil in the Cook Inlet Basin of Alaska was completed in 1957. Estimated amounts of recoverable oil by conventional methods total 2.7 billion barrels, or 36 percent of the estimated oil originally in place. Repressurization by injecting gas or water in formations containing undersaturated oil has significantly increased the volume of recoverable oil.

The CIB oils are low in sulfur and contain low to moderate amounts of asphalt. They are also characterized as high gravity crudes (35°API) and typically have high nitrogen content, with produced surface gases as high as 15 mole percent nitrogen. In general, crudes having high nitrogen content also have high sulfur content; CIB crudes are highly unusual in that the nitrogen content exceeds the sulfur content.

The high non-hydrocarbon gases of both the ANS and CIB crude oils make the use of the previously published PVT correlations inaccurate.

TABLE 1

OIL AND GAS FIELDS IN ALASKA

(In Pocket)

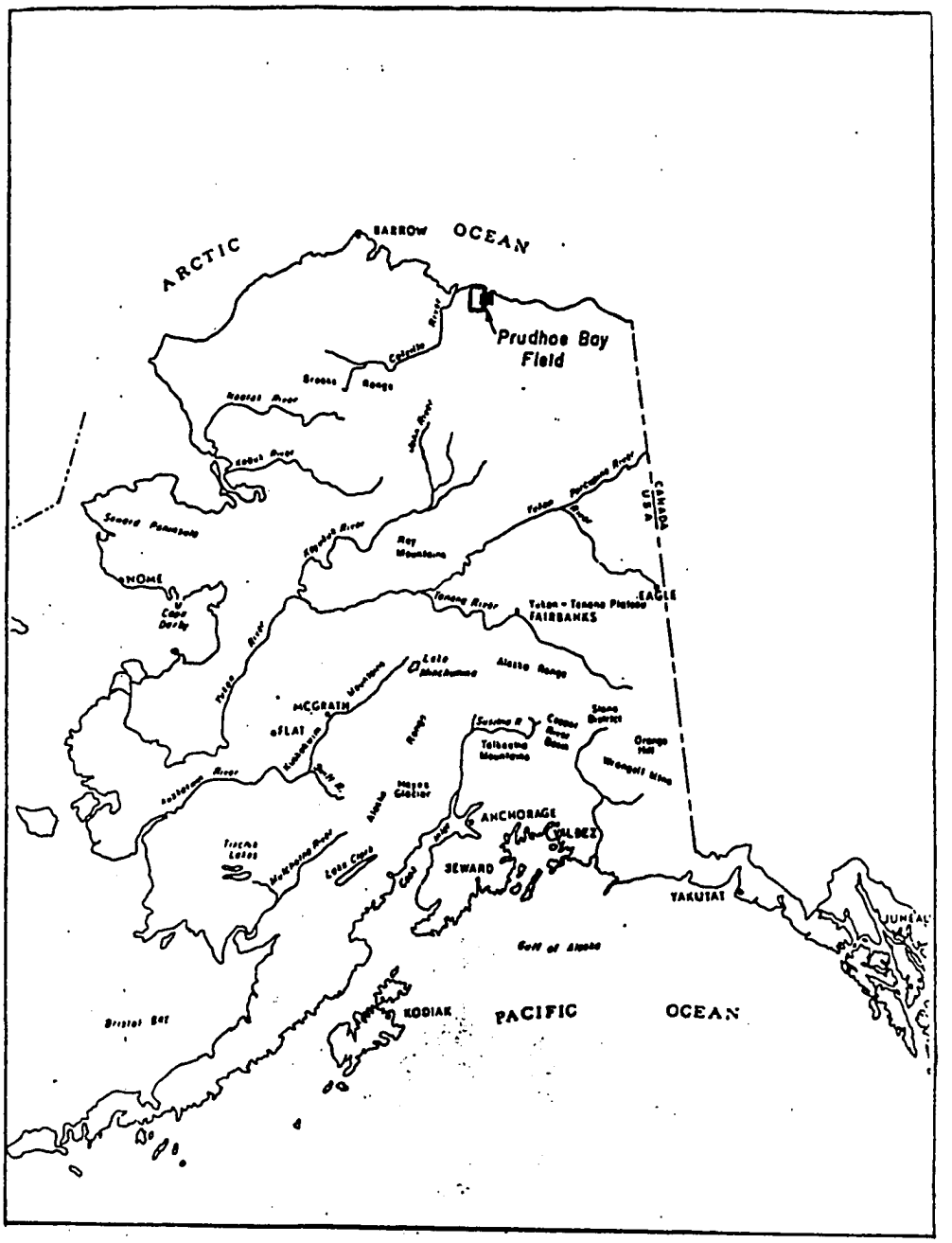

FIG. 1: LOCATION OF PRUDHOE BAY FIELD, STATE OF ALASKA

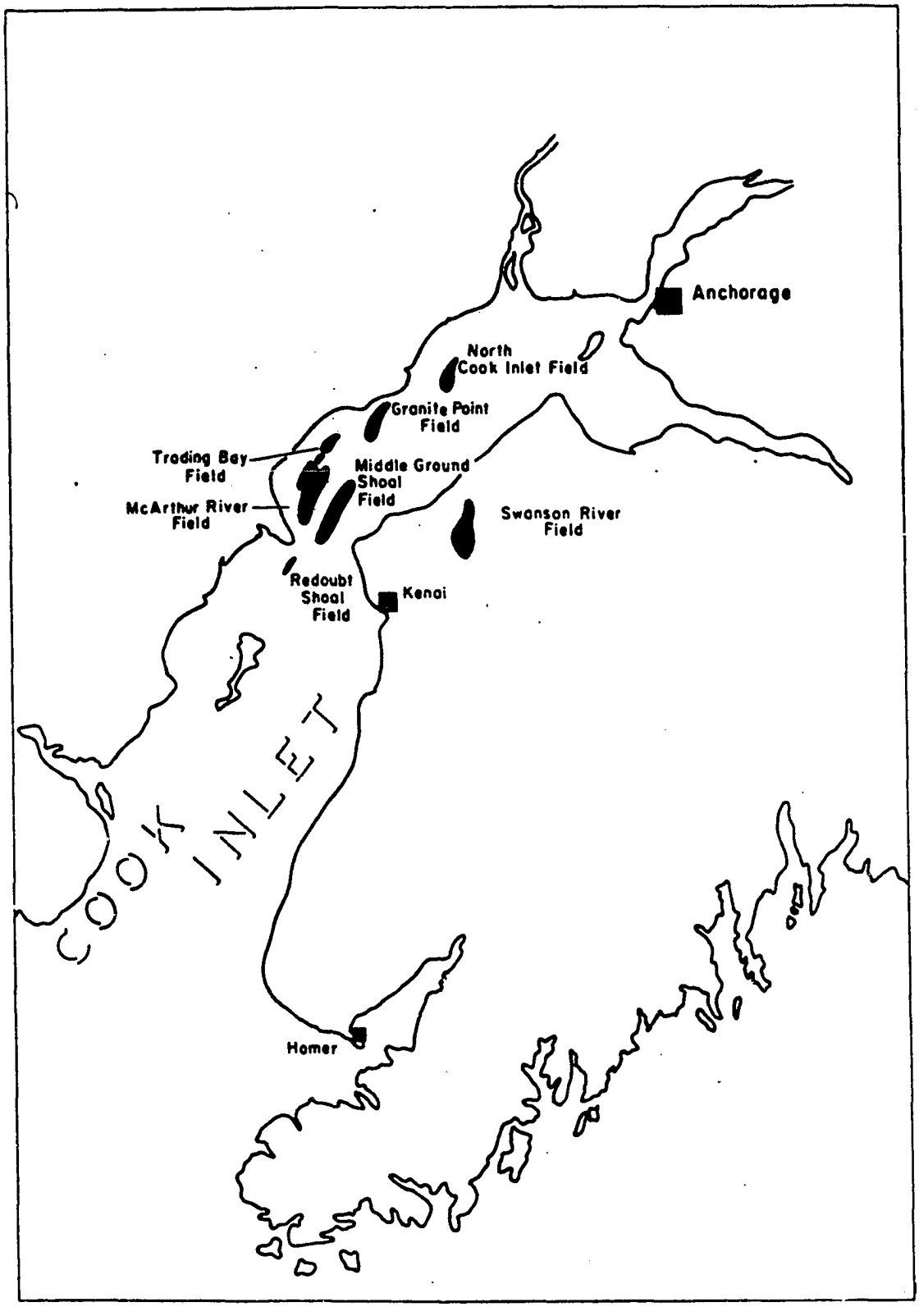

FIG. 2 : OILFIELDS IN THE COOK INLET BASIN, ALASKA

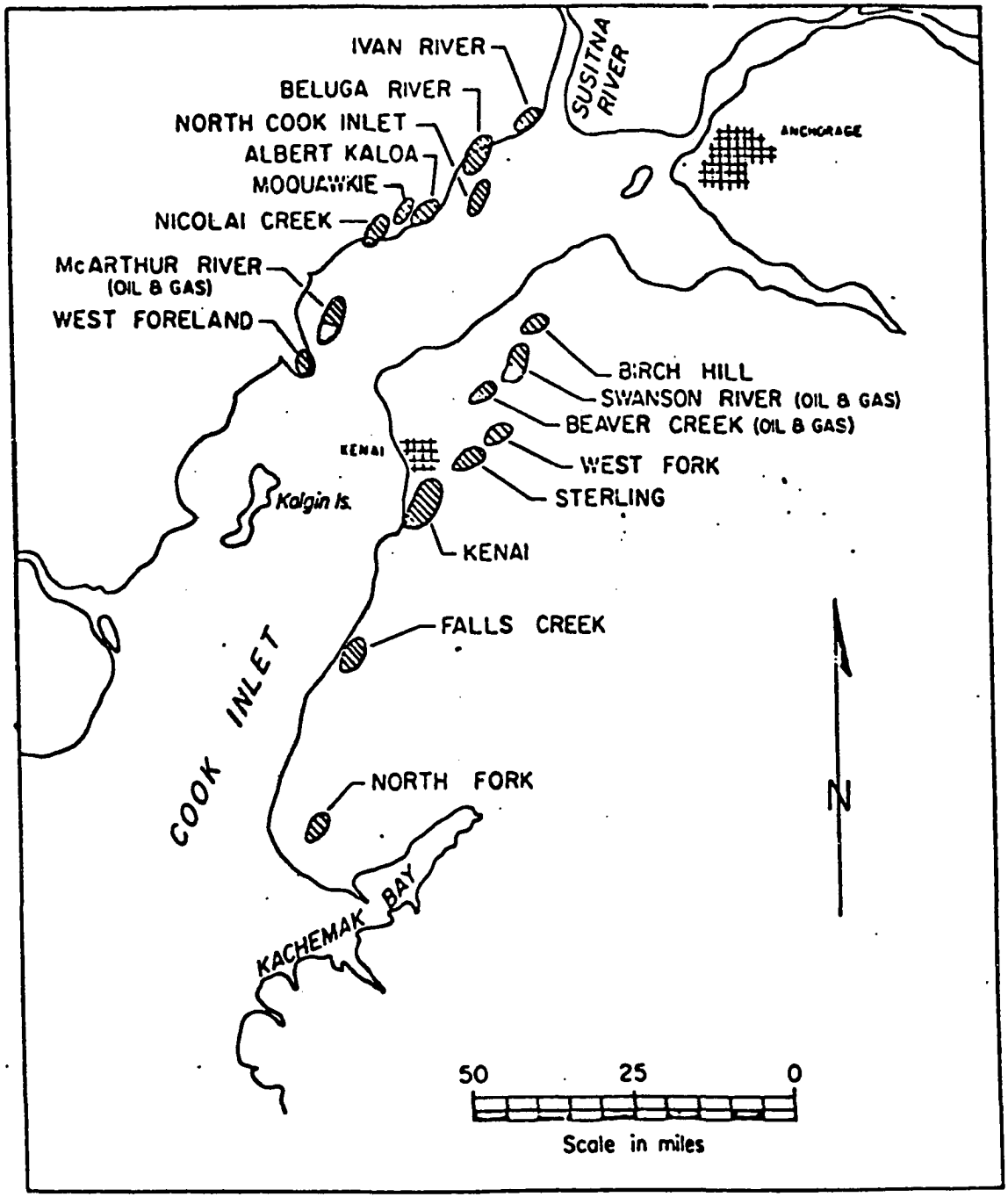

FIG. 3 : NATURAL GAS FIELDS IN THE COOK INLET BASIN, ALASKA

CHAPTER II

LITERATURE SURVEY

Various PVT correlations from which material balance calculations, ranging from simple estimations of the oil originally in place to detailed studies of the reservoir performance can be made, have been proposed in the literatures over the years. Among the existing correlations only the standing correlations have gained wide acceptance in the oil industry. However, neither the Standing's[19] nor the other correlations fit very well for the Alaskan Crudes, because of high non-hydrocarbon gases. The inspiration for this my present study came from these findings.

To use the best approach for this study, a thorough review of the presently available methods was conducted. Methods of correcting for the non-hydrocarbon contents was also looked at.

STANDING

The best known method for predicting bubble point pressure, solution gas-oil ratio and formation volume factor, was developed by Standing[19]. Standing's correlation was developed in 1947, based on analysis of PVT studies from a series of 22 different crude oil/natural-gas mixtures from California oil fields. He developed correlations for bubble point pressures, formation volume of bubble point liquids, and formation volumes of gas plus liquid phases as empirical functions of gas-oil ratio, gas gravity, oil gravity, pressure, and temperature.[19] His correlations were derived

from 105 experimental data points and make no corrections for oil type or non-hydrocarbon contents. He reported a general relationship between bubble point pressure and fluid properties in the form:

$$P_b = f_1(R_s, \gamma_g, \gamma_{API}, T) \qquad (1)$$

Likewise, for the formation volume factor of bubble point liquid, the correlating equation he developed was of the form:

$$B_{ob} = f_2 \left[R_s \left(\frac{\gamma_g}{\gamma_o}\right)^a + b.T \right] \qquad (2)$$

A thorough development of his and the other correlating equations is shown in the Appendix C. For the above and other equations, the definition of terms and the SI metric conversion factors are shown in Appendix A and Appendix B respectively.

LASATER

In 1958, Lasater[13] presented a correlation of the bubble point pressure for black oil systems, developed using the Standard physical-chemical equations of solutions. The correlation was prepared from 158 experimentally measured bubble point pressure of 137 independent crude oil systems from Canada, U.S., and South America. His correlation is expressed in terms of flash separation gas-oil ratio, tank oil gravity, total gas gravity, and reservoir temperature.

The basic assumption he used in his development is the same as employed by Standing.

Lasater's correlation has been found to be more accurate than Standing's correlation for high-gravity crude oil systems,[18] and many engineers prefer using Standing's correlation for crudes of API gravity less than 20° and the Lasater's correlation for lighter crudes.

VAZQUEZ AND BEGGS

In 1980, Vazquez and Beggs[21] presented correlation obtained by regression analysis using 5,008 measured data points from fields all over the world. He reported a general relationship between bubble point pressure and fluid properties in the form:

$$P_b = f\ (R_s, \gamma_g, T_s, P_s, \gamma_{API}, T) \qquad (3)$$

Their relationship for the oil formation volume factor, is of the form:

$$B_{ob} = f\ (R_s, \gamma_g, T_s, P_s, \gamma_o, T) \qquad (4)$$

In the development of the correlation, the measured average gas gravity for each sample was corrected to the gravity which would have been obtained if the separation had been conducted at Standard conditions of 100 psig, and

60°F. This corrected gravity (γ_{gs}), was calculated from a correlation based on the actual separator conditions and the measured gas gravity. For details of equations for the correlations, refer to Appendix C. The Vazquez and Beggs correlation has been adopted by Hewlett-Packard for use in the HP 41-C Petroleum Fluids Pac.

GLASO

Glaso[8], in 1980, presented empirical equations for estimating saturation pressure, oil formation volume factor at saturation pressure and two-phase formation volume factor, derived as a function of reservoir temperature, total surface-gas gravity, producing gas oil ratio and stock-tank oil gravity. His correlations are based on laboratory data from North Sea crudes, and they are supposed to be valid for all types of oil/gas mixtures after correcting for non-hyrocarbons in surface gases and paraffinicity of oil. The Glaso correlation is of the form:

$$P_b = f\ (R_s,\ \gamma_g,\ \gamma_{API}\ ,\gamma_{API,\ corr.},\ T) \qquad (5)$$

where, $\gamma_{API,\ corr.}$ is a corrected value for the stock tank oil gravity based on the paraffinicity of the crude oil. The calculation of $\gamma_{API,\ corr.}$ requires measurement of the gravity, γ^{*}_{API}, and the viscosity, $\mu_{od,}$ of the residual oil resulting from differential liberation of reservoir temperature.

Glaso[8] also reported correction factors for the effect of non-hydrocarbons, like nitrogen, carbon-dioxide and hydrogen sulfide, on bubble point pressure. The corrections are multiplication factors to be applied to the bubble point pressure as:

$$P_{b,\ corr.} = CP_b \qquad (6)$$

Also, refer to Appendix C for detailed development of his equations.

JACOBSON

In 1967, Jacobson[9] presented correlations of correction factors for the effect of nitrogen on the bubble point pressure of reservoir fluids. His work was based on series of measurements made in the laboratory and through references to bubble point pressure correlations in the literature, and was intended for use with Standings [19] correlation.

Among the reservoirs Jacobson studied, mostly from fields located in Alberta, Canada, he noticed that the nitrogen content of solution gases tends to decrease as reservoir temperature increases. He developed the following linear equation to adjust bubble point pressure correlation for the effect of nitrogen:

Adjustment = 15.85+2.86 x Nitrogen - 0.107 x temperature

(7)

BEGGS AND ROBINSON

Beggs and Robinson[2], in 1975 presented correlation to estimate the viscosity of crude oil systems based on laboratory PVT analyses of reservoir fluid samples. They developed empirical correlations for dead or gas-free crude oil as a function of API gravity and temperatures, and for live oil viscosity as a function of dissolved gas and dead oil viscosity.

The expression developed for the dead oil viscosity was:

$$\mu_{od} = 10^{Z} - 1 \qquad (8)$$

Where:

$$Z = T^{-1.163}\ 10^{(3.0324-0.02023\gamma API)} \qquad (9)$$

Live oil viscosity at or below the bubble point pressure can be estimated from:

$$\mu_{ob} = A\ \mu_{od}^{\ B} \qquad (10)$$

Where:

$$A = 10.715\ (R_s + 100)^{-0.515} \qquad (11)$$

and,

$$B = 5.44\ (R_s+150)^{-0.338} \qquad (12)$$

Live oil viscosity above the bubble point is estimated as:

$$\mu_o = \mu_{ob}\ (p/p_b)^m \qquad (13)$$

Where:

$$m = 2.6\ p^{1.187}\ EXP\ (-8.98\ X\ 10^{-5}p - 11.513) \qquad (14)$$

BEAL

In one of the early works found in the literature, Beal[1] in 1945 presented correlations for dead oil viscosity. He also developed a correlation for viscosity of undersaturated crude oils. The Beal correlation for gas-free or dead oil viscosity is used widely throughout the oil industry and is considered to be fairly accurate. The limitations found in his presentation is the lack of analytical expressions to evaluate viscosities of crude oil systems below and above the bubble point.

The literature review reveal that most widely used correlations for estimating bubble point pressure, oil formation factor, solution gas-oil ratio and oil viscosity, made use of data from a specific geographical region in the

development of correlations. Therefore a lot of deviation occurs in predictions obtained when extrapolating the correlations for use on crudes of different characteristics.

CHAPTER III

THE EFFECT OF NON-HYDROCARBON GASES ON RESERVOIR FLUID PROPERTIES OF ALASKAN CRUDES

INTRODUCTION

The effect of non-hydrocarbon gases on reservoir fluid properties, like bubble-point pressure, formation volume factors and solution gas-oil ratio can range from minimal to extreme, depending on the type of non-hydrocarbon gas content, the quantity with which it is found in the reservoir oil, temperature and stock-tank oil gravity. The common non-hydrocarbon gases affecting the behavior of reservoir fluid properties are nitrogen, carbon dioxide and hydrogen sulfide.

The present study was accomplished by first gathering laboratory reservoir fluid properties analyses from oil fields in Alaska. A thorough study of Alaskan crudes system indicated that the reservoir fluid properties do not agree with the published correlations. Due to unavailability of separator gas content analyses of data from Alaskan North Slope, this discussion is mainly restricted to the effect of nitrogen on Cook Inlet Basin crude oils system. Due to the presence of the non-hydrocarbon gases, the published correlations predicted values that were too low for bubble-point pressure, solution gas-oil ratio and the formation

volume factor at bubble-point. Addition to the predicted bubble-point pressure increases as the temperature and methane content decrease. Whereas addition to the predicted formation volume factor at bubble point increases as the temperature and methane content increase. Discrepancies of up to 35 percent were observed for the bubble-point pressure and up to about 10 percent for the formation volume factor at bubble-point pressure. Since the correlations for bubble-point pressure are normally rearranged to give correlations for the solution gas-oil ratio at bubble-point, discrepancies of up to 35 percent would also be observed for the solution gas-oil ratio.

The bubble-point pressure, is an important property of a reservoir fluid. This pressure, being equal to the measured formation pressure indicates that the reservoir oil is saturated with gas and that a gas cap is very likely to be present. When the bubble-point pressure is less than the measured formation pressure, this indicates an undersaturated reservoir, one that could absorb an additonal volume of gas. The volume of gas that the under-saturated reservoir might absorb would depend on the solubility of the gas made available to it. The solubility of naturally occuring hydrocarbon gases increases with their molecular weight.

Nitrogen influences saturation pressure in two ways. Due to low solubility of nitrogen gas in the liquid phase of hydrocarbons, higher pressures are required to force the

nitrogen gas into solution. Also, the pressure-temperature phase diagram at bubble-point (saturation) pressure has a lower slope than in a system without nitrogen. Based on these facts, correction factors for nitrogen gas content on the bubble-point pressure, have been proposed by Jacobson[9] and Glaso[8].

For systems containing large quantities of carbon dioxide one would, according to Lasater[13], have higher bubble-point pressures than calculated from the published PVT correlations since carbon dioxide is less soluble in oil than are hydrocarbon gases. But Glaso[8] proposed that the effect of CO_2 gas has the opposite influence on bubble-point pressure. Glaso also reported that for systems containing large quantities of hydrogen sulfide gas, the bubble point pressures would be lower than those predicted from the published PVT correlations.

RESULTS AND DISCUSSION

For reasons mentioned earlier in this chapter, the discussion is going to focus mainly on the effects of non-hydrocarbon gas contents, and on the reservoir properties of the Cook Inlet Basin crude oils system. Although the data on which the study is based are limited, it does indicate the range of reservoir fluid properties variation that may be attributed to nitrogen.

The map on Figure 2, locates some of the fields in the Cook Inlet Basin, Alaska, that are represented in the

study. The solution gases contain up to 15 percent nitrogen as well as about 0.20 percent carbon dioxide (Table 2). To illustrate the low solubility of nitrogen in oil, a correlation between the nitrogen content of separator gas and the ratio between methane and nitrogen was used (Figure 4). The same was done for carbon dioxide content (Figure 5), to illustrate the solubility of carbon dioxide in oil. For example at the reservoir temperature of 180°F, the trend indicates that where the field separator gas contains 5 percent nitrogen gas, the methane and nitrogen will be in the ratio of 15.7 to 1. At 0.2 percent carbon dioxide gas content, for example, the methane and carbon dioxide will be in the ratio of 398 to 1 (Figure 5) and the nitrogen and carbon dioxide will be in the ratio 31 to 1 (Figure 6).

Due to the very low amount of carbon dioxide gas in Cook Inlet Basin oils system, the remaining part of the discussion deals with only the effect of nitrogen gas content on reservoir fluid. Figures 7 through 10, represent correlations showing the influence of field separator nitrogen gas content on reservoir properties like bubble-point pressure, solution gas oil ratio, formation volume factor at bubble-point and live oil viscosity at bubble-point.

The correlations between nitrogen content and both bubble-point pressure and solution gas-oil ratio, were plotted on a log-log coordinate system. They both showed a linear trend until the effect of reservoir temperature

started becoming noticeable at about 10 mole percent nitrogen. For futher study of these effects, predictions of bubble-point pressures using the published PVT correlations for bubble-point pressure was looked at. As shown in Table 3, Standing[19], Vazquez-Beggs[21], Glaso[8] and Lasater[13] correlation, resulted in discrepancies of up to 35 percent. Most of the predicted bubble-point pressure values were too low and the bubble-point pressure nitrogen gas content correction factors required were found to increase as the temperature and methane content decrease (Tables 2,3, and 4).

For the case of formation volume factor at bubble-point, the influence of nitrogen gave a linear trend at varing temperatures, on a cartesian plot. Predictions of formation volume factor at bubble-point using the published correlations 19,21,8, resulted in discrepancies of up to about 10 percent (Table 7). In this case also, most of the predicted values were too low and the formation volume factor at bubble-point nitrogen gas content correction factors required was found to increase as the temperature and methane content increase (Tables 2 and 7).

Lastly, for the case of live oil viscosity at bubble-point, the influence of nitrogen content also gave a linear plot on a log-log coordinate system as shown in Figure 10. Predictions of live oil viscosity at bubble-point using the published correlations[1,2], resulted in discrepancies of up to about 20 percent. At a temperature of 152°F, the

TABLE 2

PVT PROPERTIES OF COOK-INLET BASIN CRUDE OILS

SAMPLE	T_s (°F)	p_s (psia)	γ_g	γ_{API} (°API)	Y_{C1} (*) (%)	Y_{N_2} (*) (%)	Y_{CO_2} (*) (%)	T (°F)	R_s ($\frac{Scf}{STB}$)	p_b (psia)	B_{ob} ($\frac{Res.Bbl.}{STB}$)	μ_{ob} (cp)	μ_{od} (cp)
1.	60	165	0.911	35.0	66.55	14.77	0.13	152	288	1637	1.185	1.05	2.48
2.	60	165	0.955	35.3	69.80	9.92	0.16	152	224	1159	1.160	1.13	2.48
3.	60	165	1.094	34.9	71.50	4.67	0.23	152	140	515	1.129	1.32	2.48
4.	60	165	0.853	35.2	70.32	13.40	0.13	180	306	1782	1.199	0.90	2.10
5.	60	165	0.888	34.9	73.88	10.45	0.14	180	236	1263	1.179	1.00	2.10
6.	60	165	1.020	32.7	78.00	4.79	0.19	180	140	565	1.144	1.33	2.10
7.	60	104	0.878#	35.4	62.40	15.10	N/A	180	309	1802	1.205	0.96	2.05

* Separation gas

\# Stock tank gas gravity calculated from separator liquid flash

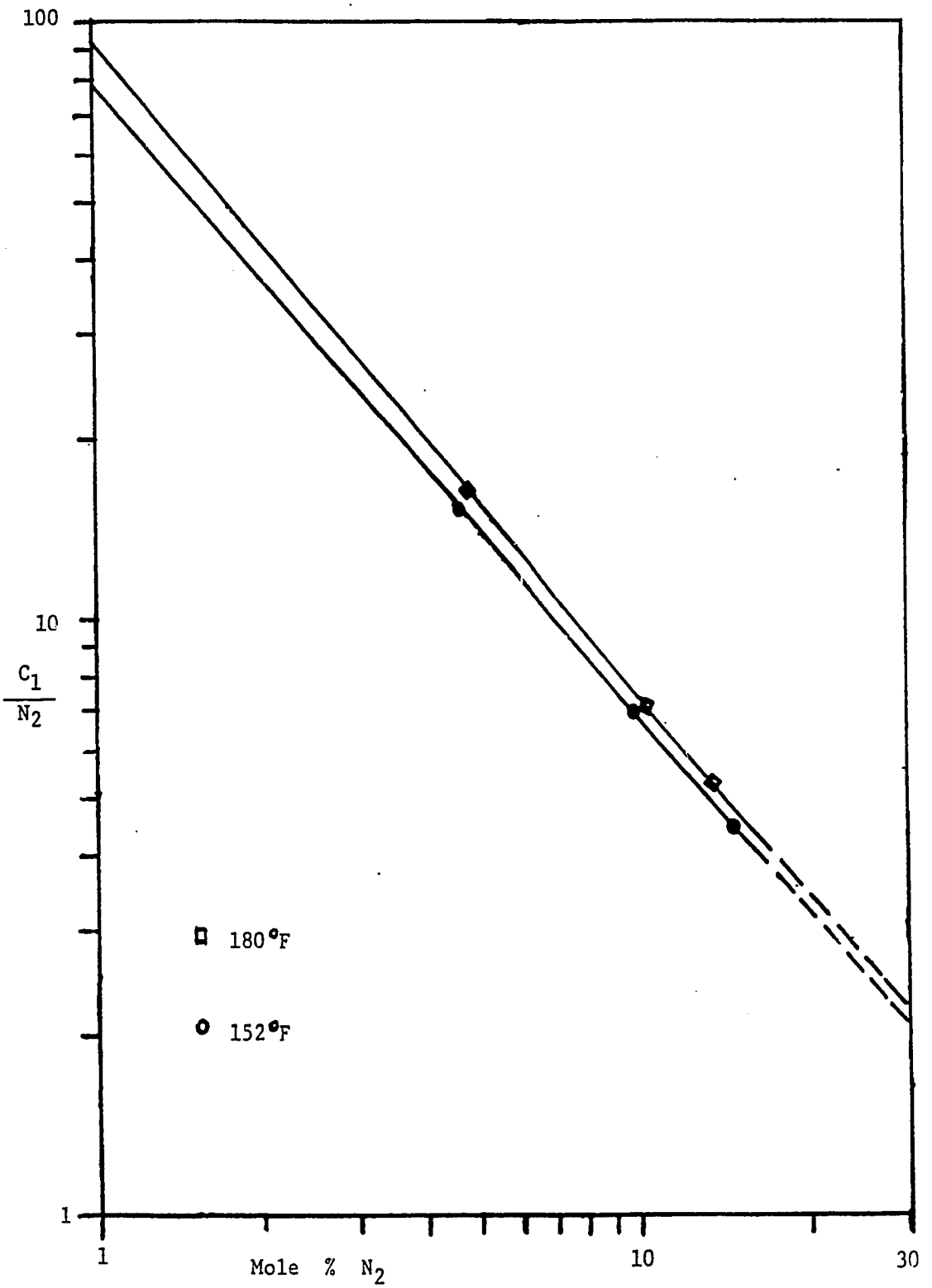

FIG. 4 : FIELD SEPARATOR GAS, METHANE-NITROGEN RATIO VS. NITROGEN CONTENT FOR COOK INLET BASIN, ALASKA HYDROCARBON SYSTEMS

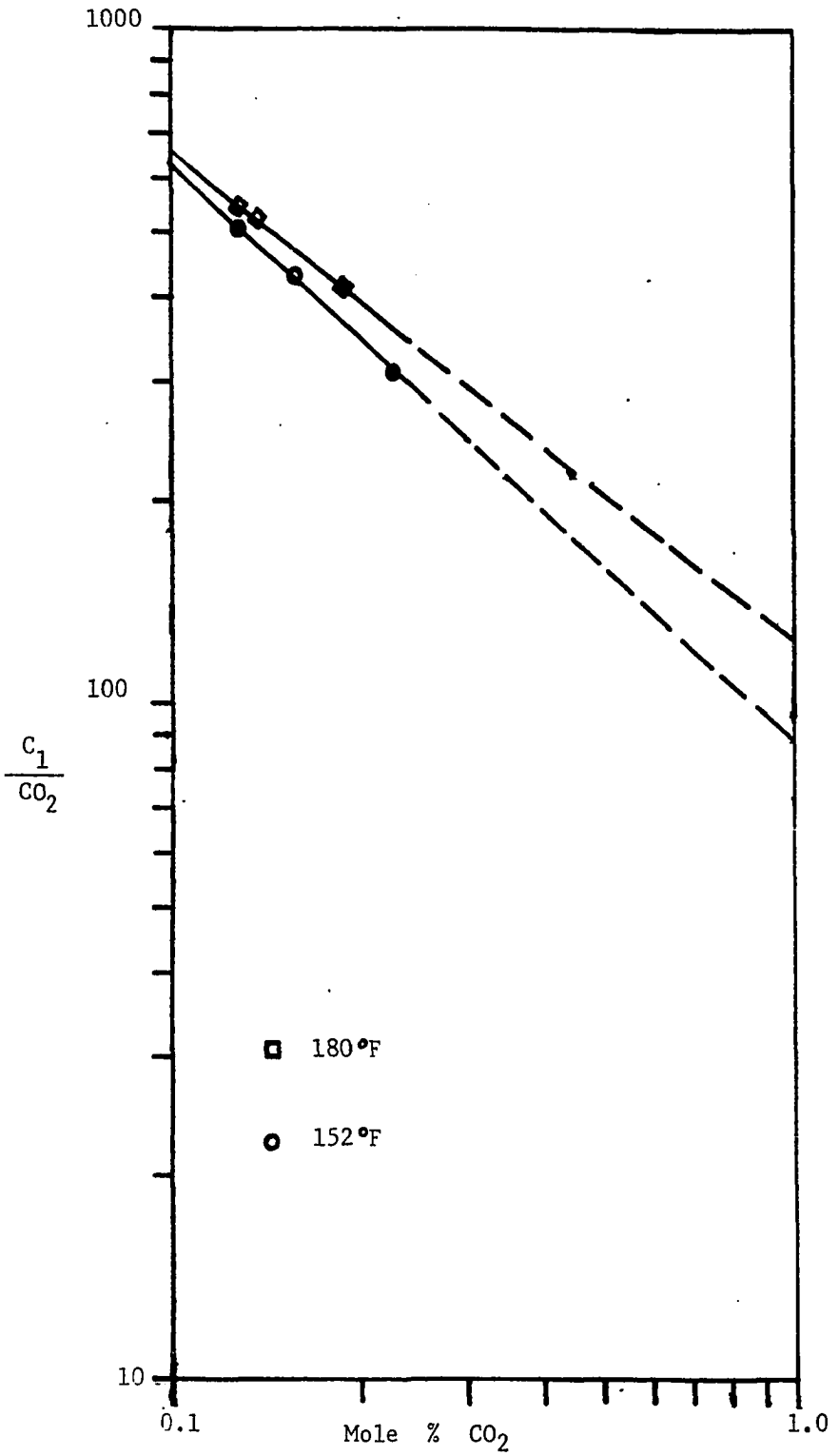

FIG. 5 : FIELD SEPARATOR GAS, METHANE-CARBON DIOXIDE RATIO VS. CARBON DIOXIDE FOR CIB HYDROCARBON SYSTEMS

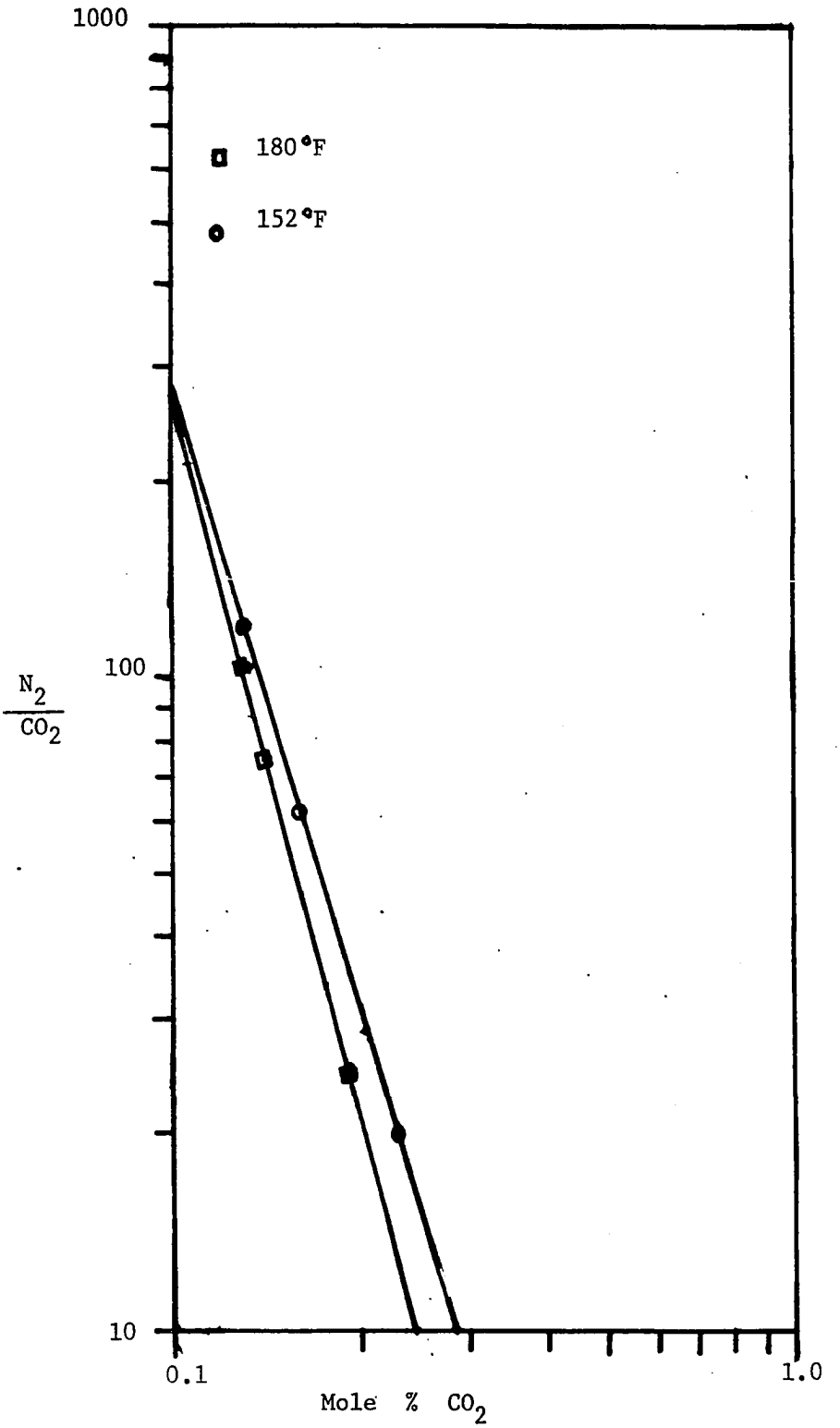

FIG. 6 : FIELD SEPERATOR GAS, NITROGEN-CARBON DIOXIDE RATIO VS. CARBON DIOXIDE FOR CIB HYDROCARBON SYSTEMS

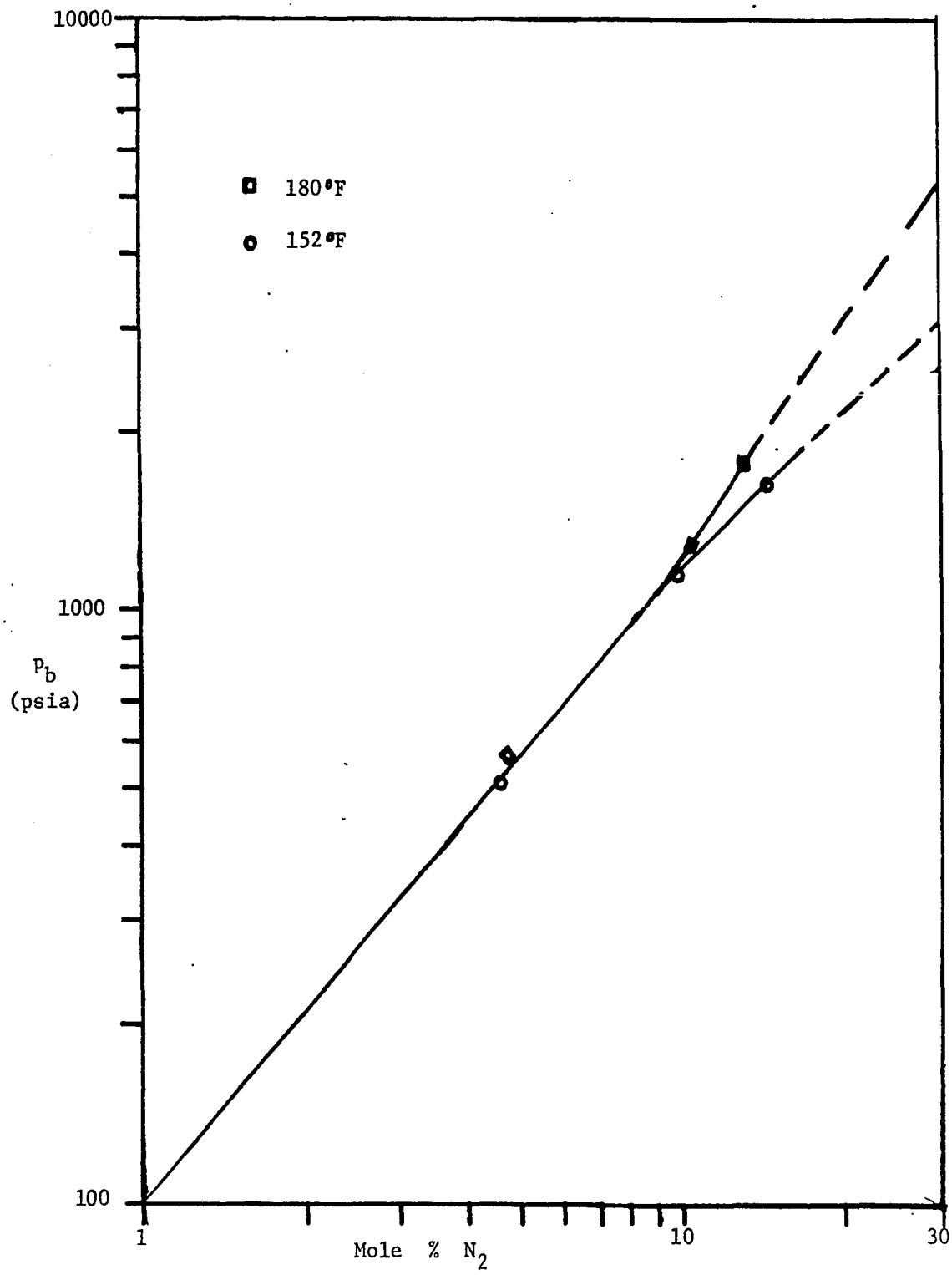

FIG. 7 : BUBBLE-POINT PRESSURE VS. FIELD SEPARATOR GAS NITROGEN CONTENT FOR CIB HYDROCARBON SYSTEMS

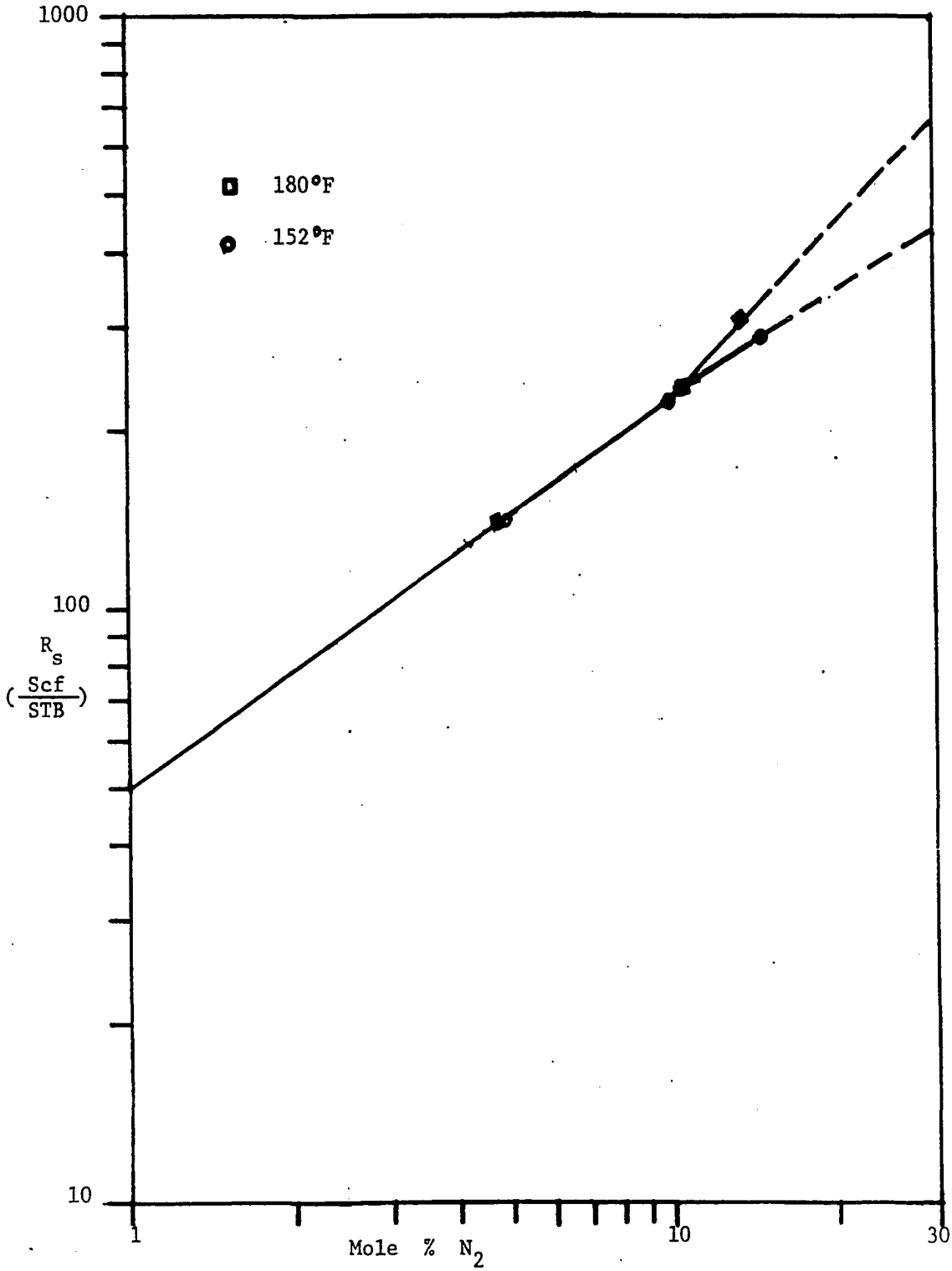

FIG. 8 : SOLUTION GAS-OIL RATIO VS. FIELD SEPARATOR NITROGEN CONTENT FOR CIB HYDROCARBON SYSTEMS

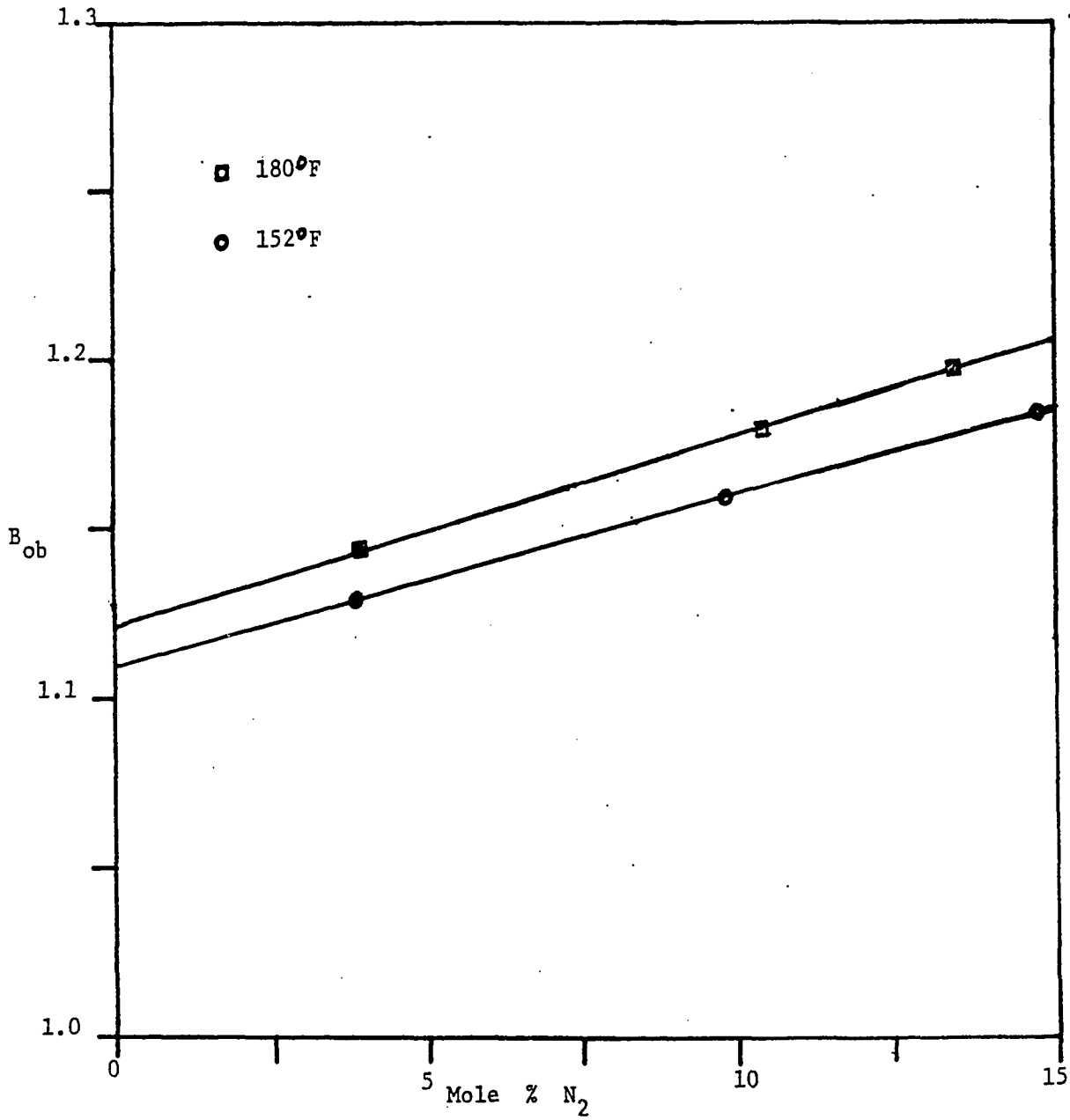

FIG. 9 : OIL FORMATION VOLUME FACTOR AT BUBBLE-POINT VS. FIELD SEPARATOR NITROGEN CONTENT FOR CIB HYDROCARBON SYSTEMS

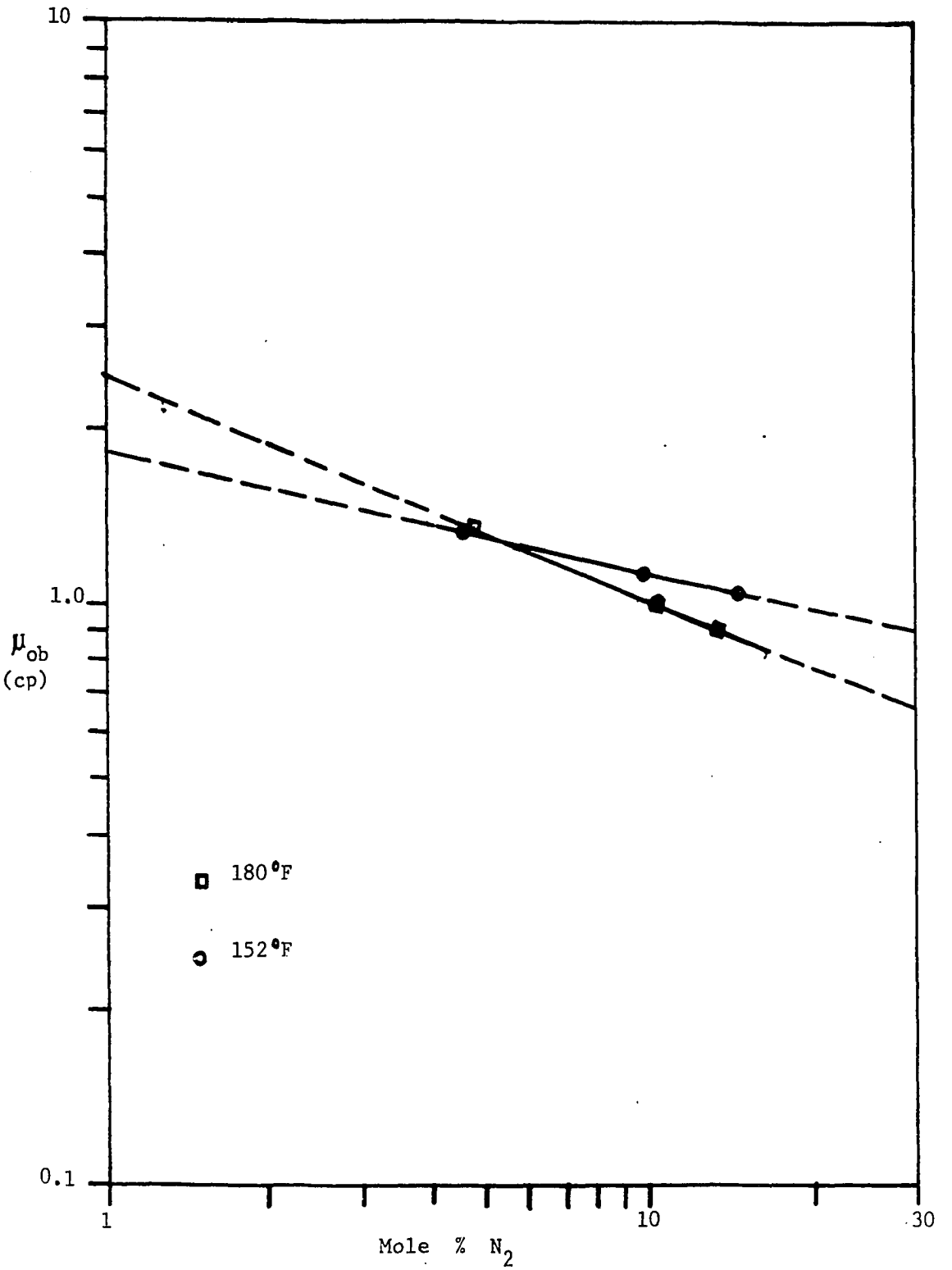

FIG. 10 : LIVE OIL VISCOSITY AT BUBBLE-POINT VS. FIELD SEPARATOR GAS NITROGEN CONTENT FOR CIB HYDROCARBON SYSTEMS

CHAPTER IV

ALASKAN CRUDE OILS PVT CORRELATIONS

INTRODUCTION

Laboratory data on bubble-point pressures, oil formation volume factors and oil viscosities have been correlated as functions of solution gas-oil ratio, gas gravity, oil gravity and reservoir temperature.

The high non-hydrocarbon contents of both Alaskan North Slope and Cook Inlet Basin crude oils call for the development of PVT correlations for Alaskan hydrocarbon systems. Apart from Glaso's[8] correlations, all the presently published correlations were based on non-hydrocarbon free systems.

Generally, laboratory reservoir fluid property tests furnish information on solution gas oil ratios, residual oil gravities, bubble-point pressure, oil formation volume factors, viscosities of oils and occasionally gas gravities. Each kind of data has its own applications and use in reservoir engineering calculations. The particular uses of correlated PVT data are found in:

1. Providing a basis for obtaining predictions of reservoir fluid properties in fields where the laboratory PVT reports are unavailable.
2. Greatly reducing the time in obtaining the desired information.
3. Serving as a check on data which may appear out of line.

4. Predicting original or other properties of reservoirs that were not sampled in the past.

PROCEDURES

Application of the previously published correlations [1,2,8,13,19,21] to the laboratory PVT data of Alaskan crude oils indicated that they do not fit well. This inspired the present study, making use of PVT reports from fields in Alaska. For the Cook Inlet Basin correlations, two of the PVT reports included combined differential and flash separations which effectively created four additional bubble-point fluids, thus expanding the sample to seven fluids.

The variables from available laboratory data are defined below.

1. Bubble-Point Pressure: This is the pressure at which there is a break in slope of the pressure-volume curve; that is the pressure at which gas starts to evolve as pressure is decreased. This bubble-point pressure is at the test temperature.
2. Solution Gas-Oil Ratio: The volume ratio obtained by dividing the amount of gas which would be liberated from a system existing originally as a liquid, by the liquid remaining after the system is reduced to standard atmospheric conditions of 14.7 psia and 60°F.

3. Oil Formation Volume Factor: This is the barrels of bubble-point oil per barrel of residual oil at 60^{0}F and atmospheric pressure. Separation of gas is by flash process at reservoir temperature.
4. Oil Viscosity: Viscosity is a measure of flow resistance. The viscosity of a liquid or gas is important because it is a measure of its fluidity, or its ability to flow through pipe lines or oil sands. The viscosity of gas-saturated crude oil at reservoir pressure and temperature is measured using one of the many types of viscosimeters, and is of particular value in making estimates of oil reserves.
5. Gas Gravity: Ratio of the molecular weight of the gas to the molecular weight of air.
6. Oil Gravity: This is the API gravity of the residual oil. The gravity is measured at room temperature and corrected to 60^{o} F .
7. Temperature: This is the temperature at which the differential, flash seperations and bubble point pressure determinations are carried out, and is usually the bottom hole (reservoir) temperature.

RESULTS AND DISCUSSION

Bubble-Point Pressure Correlations:

The basic assumption used in this development is the same as reported by Standing[19], for the general relation

between bubble-point (saturation) pressure of an oil and gas system with its fluid and reservoir properties.

$$P_b = f_1 (R_s, \gamma_g, \gamma_{API}, T) \qquad (1)$$

COOK-INLET BASIN

Using graphical methods and regression analysis, the following relations were developed from the data (Table 2) for Cook Inlet Basin Oils.

$$(P_b)_{T,\ \gamma_{API}} = h_1 \left(\frac{R_s}{\gamma_g}\right)^{1.255} \qquad (15a)$$

$$\frac{P_b}{\left(\frac{R_s}{\gamma_g}\right)^{1.255}} = h_2 \cdot T^{0.172} \qquad (15b)$$

$$\frac{P_b}{\left(\frac{R_s}{\gamma_g}\right)^{1.255} \cdot T^{0.172}} = h_3 \cdot \gamma_{API}^{-0.178} \qquad (15c)$$

Hence,

$$P_b = h_3 \cdot \left[\left(\frac{R_s}{\gamma_g}\right)^{1.255} \cdot \frac{T^{0.172}}{\gamma_{API}^{0.178}}\right] \qquad (15d)$$

To obtain the relationships expressed in equation (15d) it was necessary to make a plot of data obtained from the equation versus the experimental data for CIB crude oils. These were plotted on a log-log coordinate system, resulting in a linear trend (Fig. 11). Futher application of

regression analysis on these data, resulted in the following equations:

$$P_b = 55.0 + 0.8643\ P_b^* \qquad (16a)$$

where,

$$P_b^* = \left(\frac{R_s}{\gamma_g}\right)^{1.255} \cdot \frac{T^{0.172}}{\gamma_{API}^{0.178}} \qquad (16b)$$

ALASKAN NORTH SLOPE

Due to the lack of complete PVT reports from the Sadlerochit Formation, Prudhoe Bay field, the ANS correlation is mainly based on data from Kuparuk River Formation, Prudhoe Bay field (Table 9). Using graphical methods and regression analysis, the following relations were developed from the data for Alaskan North Slope Oils.

$$(P_b)_{T,\gamma_{API}} = h_4 \left[\frac{R_s}{\gamma_g}\right]^{0.502} \qquad (17a)$$

$$\frac{P_b}{\left(\frac{R_s}{\gamma_g}\right)^{0.502}\ \gamma_{API}} = h_5 \cdot T^{0.052} \qquad (17b)$$

$$\frac{P_b}{\left(\frac{R_s}{\gamma_g}\right)^{0.502} \cdot T^{0.052}} = h_6 \cdot \gamma_{API}^{-0.177} \qquad (17c)$$

Hence,

$$P_b = h_6 \cdot \left[\left(\frac{R_s}{\gamma_g}\right)^{0.502} \cdot \frac{T^{0.052}}{\gamma_{API}^{0.177}}\right] \qquad (17d)$$

Using data from equation (17d) and from the experimental data for ANS crude oils, a linear trend (Fig.17) was obtained on a log-log coordinate system. Application of regression analysis on these data resulted in the following equations:

$$P_b = 350\ P_b^* - 1204 \qquad (18a)$$

where,

$$P_b^* = \left[\frac{R_s}{\gamma_g}\right]^{0.502} \cdot \frac{T^{0.052}}{\gamma_{API}^{0.177}} \qquad (18b)$$

In all the equations, oilfield units are used as shown in Appendix A. The term P_b^* is the "correlating number" to calculate bubble-point pressure.

The above Equations (15d) and (17d), were developed into nomographic form (Figs. 14 and 20) for further simplicity and for use in the field. The nomographic correlation is based on the equations below:

$$f_a(P_b) = f_b\left[\frac{R_s}{\gamma_g}\right] \cdot f_c(T) \cdot \frac{1}{f_d(\gamma_{API})} \qquad (19a)$$

Let,

$$\partial = \frac{f_b\left(\frac{R_s}{\gamma_g}\right)}{f_d\left(\gamma_{API}\right)} \qquad (19b)$$

Then,

$$f_a(P_b) = f_c(T) \cdot \partial \qquad (19c)$$

and each of the three-variable equations can be handled by converting to the logarithmic forms,

$$\log \partial = \log f_b\left[\frac{R_s}{\gamma_g}\right] - \log f_d\left[\gamma_{API}\right] \qquad (19d)$$

and,

$$\log f_a[P_b] = \log f_c(T) + \log \partial \qquad (19e)$$

Using the basic concept of nomograph, a chart is prepared for Eq. (19b), the ∂ axis lying between the R_s/γ_g and γ_{API} axes. Using the same ∂ axis, which need not be graduated, a similar chart is constructed for Eq. (19c) with the P_b axis between the T and ∂ axes, as in figs. 14 and 20.

COMPARISON OF THE p_b CORRELATIONS:

COOK-INLET BASIN

As shown in Table 2, the range of the data for the new CIB P_b correlation, was as follows:

Bubble-point pressures	515 to 1802 psia.
Temperature	152 to 180°F
Gas-Oil ratios	140 to 309 Scf/STB.
Tank Oil gravities	32.7 to 35.4 °API
Gas gravities	0.853 to 1.094 (air=1).

The mean error ($\bar{\chi}$) and the standard deviation (S_x), of the widely used correlations were compared to the newly developed Alaskan correlations.

$$\bar{\chi} = \frac{1}{n} \cdot \sum_{i=1}^{n} \left[\frac{Xexp. - Xpred.}{Xexp.} \right] \cdot 100 \qquad (20a)$$

$$S_x = \pm \frac{\left[\sum_{i=1}^{n} \left[\frac{Xexp. - Xpred.}{Xexp.} \right] .100 \right]^2]^{0.5}}{n-1} \qquad (20b)$$

For the Cook Inlet Basin fields, mean errors and Standard deviations of close to 30 percent respectively, were obtained using the previous P_b correlations, as shown in Table 3. With the application of Glaso's[3] nitrogen correction factors and the Jacobson's[9] nitrogen correction factors (Table 4), some improvement were obtained (Table 5). Note that since the correction factors are

multiplicative, they can be used with any of the correlations, and are not restricted to use with Standing[19] and Glaso[8]. As mentioned earlier, all the correlations perform reasonably well after correction for nitrogen. However, the Jacobson[9] correction is better for the Cook Inlet crudes.

As shown in Table 5, Glaso's[8] correlation (with Jacobson correction factor) is superior, compared to the previous correlations listed in that particular table. The mean error was more than minus 2 percent and the standard deviation was more than 5 percent.

With the newly developed CIB bubble-point correlation, a remarkable improvements resulted with a mean error of less than 1 percent and a standard deviation of about 5 percent. Since this correlation is based on Cook-Inlet Basin crude oils, no nitrogen correction factors are needed. Refer to Table 6 for bubble-point pressure predictions using the new CIB P_b correlation, on data of Table 2.

ALASKAN NORTH SLOPE

As shown in Table 9, the range of the data for the new ANS P_b correlation, was as follows:

Bubble-point pressures	2480 to 4507 psia.
Temperature	145 to 220°F
Gas-Oil ratios	341 to 850 Scf/STB.
Tank Oil gravities	18.9 to 28.4 °API.

Gas gravities 0.663 to 0.759 (air=1)

Samples 1 through 17 (Table 9), are data from Kuparuk River formation of Prudhoe Bay Field and samples 18 through 20 are data from Sadlerochit Formation of Prudhoe Bay Field. As mentioned earlier, data form Sadlerochit Formation were not included in the comparison, because of unavailabilty of complete PVT reports from reservoirs on that formation.

For the Alaskan North Slope fields, mean errors and standard deviations of more than 20 percent respectively were obtained (Table 10) using Glaso's[8] correlation. Among the previous correlations, Standing's[19] was superior for ANS crude oils, with mean error of minus 4.58 percent and standard deviation of 6.14 percent. It should be noted that no correction factors were applied to the previous correlations. This was because the PVT report obtained from the Alaskan North Slope fields did not include analysis for the separator gas content.

With the newly developed ANS bubble-point correlation, improvements resulted, with a mean error of minus 2.41 percent and a standard deviation of 4.78 percent.

SOLUTION GAS-OIL RATIO CORRELATIONS:

The correlations for bubble-point pressure can be rearranged to give a correlation for solution gas-oil ratio for pressures at or below the original bubble-point. This

is possible because all conditions below the original bubble-point represent saturation conditions. Since a correction for non-hydrocarbon content is required for the bubble-point pressure (previous) correlations, a similar correction must be applied to the solution gas-oil ratio whenever any of the previous correlations is used for predictions.

COOK-INLET BASIN

Considering the newly developed CIB bubble-point pressure correlation (Eqs. 16a and 16b), the equation for the solution gas-oil ratio for CIB crude oils can be solved for, as shown below:

$$R_s = 1.12322\ \gamma_g \cdot \left[\frac{(P_b - 55.0) \cdot \gamma_{API}^{0.178}}{T^{0.172}}\right]^{0.7968} \tag{21}$$

ALASKAN NORTH SLOPE

From Equations (18a and 18b), the equation for the solution gas-oil ratio for ANS crude oils is:

$$R_s = 8.55343X10^{-6}\ \gamma_g \cdot \left[\frac{(P_b + 1204) \cdot \gamma_{API}^{0.177}}{T^{0.052}}\right]^{1.99203} \tag{22}$$

OIL FORMATION VOLUME FACTOR AT BUBBLE-POINT PRESSURE CORRELATIONS:

One of the important factors required in reservoir calculations is the oil formation volume factor at the bubble-point (saturation) pressure. The bubble-point oil formation volume factor is used for estimating the shrinkage of oil liquid volume as oil is produced from the reservoir to the surface, when the reservoir is at bubble-point conditions. For the development of the correlations, the assumptions made is based on Standing's correlation,

$$B_{ob} = f_2 \left[R_s \left(\frac{\gamma_g}{\gamma_o}\right)^a + bT \right] \qquad (2)$$

COOK INLET BASIN

Using regression analysis on the CIB crude oils data, the constants a and b are found to be a = 0.526 and b = 1.250. The data (Table 2), plotted on a log-log coordinate system, resulted in a linear trend (Fig.12). Further application of regression analysis yielded the following equations.

$$B_{ob} = 0.9871 + 4.0689X10^{-4} \; B_{ob}^{*} \qquad (23a)$$

where,

$$B_{ob}^{*} = R_s \cdot \left(\frac{\gamma_g}{\gamma_o}\right)^{0.526} + 1.250\ T \qquad (23b)$$

ALASKAN NORTH SLOPE

For ANS crude oils data, the constants a and b are found to also be a = 0.526 and b = 1.250. The data (Table 9), plotted on a log-log coordinate system, resulted in a linear trend (Fig. 18). Using regression analysis yielded the following equations:

$$B_{ob} = 0.9957 + 3.7921 \times 10^{-4} B_{ob}^{*} \qquad (24a)$$

where,

$$B_{ob}^{*} = R_s \cdot \left(\frac{\gamma_g}{\gamma_o}\right)^{0.526} + 1.250\ T \qquad (24b)$$

The same units apply for R_s, γ_g, γ_o, γ_{API}, , and T as shown in Appendix A, and B_{ob}^{*} is a "correlating number" to calculate B_{ob} as defined in Eqs. 23b and 24b.

For further simplicity of use, the above equation (2) was developed into nomographic charts. Combination multiplication and addition operations can be handled by a chart employing both logarithmic and natural scales, if

provision for suitable transition from one type of scale to another is made. Thus for the equation

$$f_a\,(B_{ob}) = f_b\,(R_s)\,.\,f_c\,(\frac{\gamma_g}{\gamma_o}) + f_d\,(T) \qquad (25a)$$

let,

$$B = f_b\,(R_s)\,.\,f_c\,(\frac{\gamma_g}{\gamma_o}) \qquad (25b)$$

Hence,

$$f_a\,(B_{ob}) = B + f_d\,(T) \qquad (25c)$$

From the application of the basic concept of nomograph, a chart is prepared for Eq. 2. One B - scale is logarithmic and the other (E-scale) is natural. Since these cannot be superimposed, it is necessary to provide guide lines connecting corresponding points on the two scales, as in Figs. 15 and 21.

COMPARISONS OF THE B_{ob} CORRELATIONS:

The newly developed Alaskan B_{ob} correlations were compared to three other widely used correlations.

COOK-INLET BASIN

Standing's[19], Vazquez and Beggs[21], and Glaso's[8] correlations predicted values for formation volume factor at bubble-point, with mean errors which were too low by about 1-4 percent. The standard deviations ranged from 1.138 percent to 4.344 percent, as shown in Table 7.

With the new CIB B_{ob} correlation, remarkable improvements resulted, with a mean error of less than 0.10 percent and standard deviation of less than 0.20 percent.

ALASKAN NORTH SLOPE

Predictions of ANS crude oils, using the previous correlations, resulted in mean errors ranging form minus 1.214 to 1.648 percent and standard deviations ranging from 0.951 to 1.852 percent.

With the new ANS B_{ob} correlation, the mean error was minus 0.185 and the standard deviation was 0.789, as shown in Table 11.

OIL VISCOSITY AT THE BUBBLE-POINT PRESSURE CORRELATIONS:

Viscosity values of crude oils and crude oils containing dissolved natural gas are required in various petroleum engineering calculations. In evaluation of fluid flow in a reservoir, the viscosity of the liquid is required at various values of reservoir pressure and at reservoir temperature. This information can be obtained from a

standard laboratory PVT analysis that is run at reservoir temperature. There are cases, however, when the viscosity is needed at other temperatures. The development of the correlations is based on:

$$\mu_{ob} = f_3 [P_b, R_s, \gamma_g, \gamma_{API}, T] \qquad (26)$$

COOK-INLET BASIN

Using the CIB crude oils data (Table 2), it was found that a graph of log μ_{ob} vs log P_b resulted in straight line with an average slope of minus 0.230. Mathematically, this gave the relationship:

$$[\mu_{ob}]_{R_s, \gamma_g, \gamma_{API}, T} = h_7 \cdot (P_b)^{-0.230} \qquad (27a)$$

After series of graphical and regression analysis attempts, it was assumed that effect of R_s, γ_g, γ_{API}, on the oil viscosity of CIB oils can be neglected. The effect of bubble-point pressure is assumed to have taken care of these parameters. A second graph of log $[\mu_{ob} \cdot P_b^{0.230}]$ vs. log T also resulted in a straight line with an average slope of minus 0.615; or expressed mathematically:

$$\mu_{ob} \cdot P_b^{0.230} = h_8 \cdot T^{-0.615} \qquad (27b)$$

Hence,

$$\mu_{ob} = h_8 \cdot [\, P_b^{-0.230} \cdot T^{-0.615} \,] \qquad (27c)$$

Equation (27c) was plotted on a log-log coordinate system, resulting in a linear curve (fig. 13). Futher application of regression analysis on this data, yielded the equations below:

$$\mu_{ob} = 6.460 + 1.125 \ln \mu_{ob}^{*} \qquad (28a)$$

where,

$$\mu_{ob}^{*} = P_b^{-0.230} \cdot T^{-0.615} \qquad (28b)$$

ALASKAN NORTH SLOPE

After series of graphical and regression analysis attempts, the relationships below were developed for ANS crude oils, using data shown in Table 9.

$$[\mu_{ob}]_{R_s,\, \gamma_g,\, \gamma_{API},\, T} = h_9 \cdot (P_b)^{-1.846} \qquad (29a)$$

$$[\mu_{ob} \cdot P_b^{1.846}]_{R_s, \gamma_g,\, \gamma_{API}} = h_{10} \cdot T^{-3.500} \qquad (29b)$$

$$\left[\mu_{ob} \cdot P_b^{1.846} \cdot T^{3.500} \right]_{R_s,\ \gamma_g} = h_{11} \cdot \gamma_{API}^{-4.520} \qquad (29c)$$

Since the effect of R_s and γ_g on the μ_{ob} of Alaskan North Slope crude oils are assumed to have been taken care of by the P_b term, they can be neglected;

Hence,

$$\mu_{ob} = h_{11} \cdot \left[P_b^{-1.846} \cdot T^{-3.500} \cdot \gamma_{API}^{-4.520} \right] \qquad (29d)$$

Data obtained from Equation (29d) were plotted on a log-log coordinate system, resulting in a parabolic curve (Fig. 19). Application of regression analysis on these data, resulted in the following equations:

$$\mu_{ob} = 1.06838 \cdot EXP\left(1.11664 \times 10^{-20} \cdot \mu_{ob}^{*}\right) \qquad (30a)$$

where,

$$\mu_{ob}^{*} = P_b^{-1.846} \cdot T^{-3.500} \cdot \gamma_{API}^{-4.520} \qquad (30b)$$

In all the equations above, oilfield units are used as shown in Appendix A. The term μ_{ob}^{*} is the "correlating number" to calculate oil viscosity at the bubble-point.

Equations 27c and 29d, were developed into nomographic charts (Figs. 16 and 22). The method of development of the ANS oil viscosity correlating chart, was the same as described for that of the P_b correlations. The three-variable equations method was utilized for the development of the CIB oil viscosity correlating chart.

$$f_a(\mu_{ob}) = \frac{1}{f_b(P_b) \cdot f_c(T)} \qquad (31a)$$

This multiplication operation may be changed into the addition form by taking logarithms of both sides;

$$\log f_a(\mu_{ob}) = -\log f_b(P_b) - \log f_c(T) \qquad (31b)$$

and the chart is developed in the form of three parallel axis.

COMPARISONS OF THE μ_{ob} CORRELATIONS:

COOK-INLET BASIN

As shown in Table 8, remarkable improvements was observed when the newly developed CIB μ_{ob} correlation was used to predict live oil and dead oil (gas-free) viscosities. For the predictions of live oil viscosity, the mean error was minus 0.52 percent and the standard deviation was 4.21 percent. For the predictions of the dead oil viscosity, the mean error was minus 1.02 percent and was 6.37 percent for the standard deviation.

With Beggs and Robinson[2] and Beal's[1] correlations, mean errors were low by about 1 to 3 percent and the standard deviations were more than 10 percent, for the predictions of the live oil viscosity. In the case of the predictions of the dead oil viscosity, their mean errors ranged from minus 5.93 percent to 13.23 percent and from 14.41 percent to 17.73 percent for the standard deviations.

ALASKAN NORTH SLOPE

Table 12 shows the comparison of the live oil viscosity predictions obtained using the available μ_{ob} correlations, to that of the experimental μ_{ob} data. Using Beggs and Robinson's[2] correlations, the mean error was low by 29.23 percent and the standard deviation was 33.35 percent. With Beal's[1] correlation, the mean error was high by 19.70 percent and the standard deviation was 31.16 percent.

Using the newly developed ANS μ_{ob} correlation, the predicted live oil viscosity had a mean error of minus 5.14 percent and standard deviation of 16.14 percent, which is well within the expecterd range.

EXAMPLE OF USE OF THE NEW CORRELATIONS

COOK INLET BASIN

As an example, consider a reservoir with the following conditions:

Formation temperature	180°F
Initial Solution gas-oil ratio	306 Scf/STB
Average gas gravity	0.853 (air = 1)
Oil gravity	35.2°API

Required to predict the values for the bubble-point pressure, the formation volume factor at bubble-point and the live oil viscosity at bubble-point.

$$\frac{R_s}{\gamma_g} = \frac{306}{0.853} = 359 \text{ Scf/STB}$$

Starting with Fig. (14), mark-off 359 Scf/STB on the R_s/γ_g scale. Next mark-off 35.2 °API on the γ_{API} scale. Draw a straight line to join the two marked-off points and note the intersection on the δ-axis. Mark-off 180°F on the T scale and draw a straight line from the intercept on δ-scale to join the marked-off point on the T scale. The intercept on the P_b scale (1782 psia), is the predicted value for the bubble-point pressure.

$$\gamma_o = 141.5/(131.5 + {}^{\circ}API)$$

$$= 141.5/ (131.5 + 35.2) = 0.849$$

Therefore,

$$\frac{\gamma_g}{\gamma_o} = \frac{0.853}{0.849} = 1.005$$

Now, using Fig. (15), connect 306 Scf/STB on the Rs scale with 1.005 on the $\frac{\gamma_g}{\gamma_o}$ scale and note the intersection with the B-axis. Follow the guide lines to the E-axis and connect the point so found with 180°F on the T-scale, reading the formation volume factor at bubble-point as 1.200 res.bbl/STB on the B_{ob} scale.

Lastly, using Fig. (16), connect the predicted value for bubble-point pressure (1782 psia) on the P_b scale with 180°F on the T-scale, reading the live oil visvosity at bubble-point as 0.9 cp on the μ_{ob} scale.

The predicted values using the new correlating equations are as shown in Tables 6 through 8.

ALASKAN NORTH SLOPE

As an example, consider a reservoir with the following conditions:

Formation temperature	154°F
Initial Solution gas-oil ratio	465 scf/STB
Average gas gravity	0.685 (air = 1)
Oil gravity	22.6 °API

Required to predict the values for the bubble-point pressure, the formation volume factor at bubble-point and the live oil viscosity at bubble-point.

$$\frac{R_s}{\gamma_g} = \frac{465}{0.685} = 679 \text{ Scf/STB}$$

Starting with Fig. (20), connect 679 Scf/STB on the $\frac{R_s}{\gamma_g}$ scale with 22.6 °API on the γ_{API} scale and note the intersection with the δ-axis. Connect the point on the δ-axis with 154°F on the T scale, reading the bubble-point pressure as 2990 psia on the P_b scale.

$$\gamma_o = 141.5/(131.5 + 22.6) = 0.918$$

Therefore,

$$\frac{\gamma_g}{\gamma_o} = \frac{0.685}{0.918} = 0.746$$

Next, using Fig. (21), connect 465 Scf/STB on the Rs scale with 0.746 on the $\frac{\gamma_g}{\gamma_o}$ scale and note the intersection with the B-axis. Follow the guide lines to the E-axis and connect the point so found with 154°F on the T-scale, reading the formation volume factor at bubble-point as 1.216 res.bbl/STB on the B_{ob} scale.

Lastly, using Fig. (22), connect the predicted value for bubble-point pressure (2990 psia) on the P_b scale with 22.6 °API on the γ_{API} scale and note the intersection with the δ-axis. Connect the point on the δ-axis with 154°F on the T-scale, reading the live oil viscosity at bubble-point as 2.52 cp on the μ_{ob} scale.

The predicted values using the new correlating equations are as shown in Tables 10 through 12.

TABLE 3

BUBBLE-POINT PRESSURES PREDICTED FROM PVT

CORRELATIONS FOR COOK-INLET BASIN CRUDE OILS

-not corrected for nitrogen content-

		PREDICTED BUBBLE-POINT PRESSURE							
	Experimental Bubble-Point pressure (psia)	Vazquez - Begg[21]		Standing[19]		Glaso[8]		Lasater[13]	
SAMPLE		P_b	% Error	P_b	% Error	P_b	% Error	P_b	% Error
1.	1637	1180	-27.92	1060	-35.25	1177	-28.10	1059	-35.31
2.	1159	908	-21.66	815	-29.68	860	-25.80	783	-32.44
3.	515	552	+ 7.18	488	- 5.24	450	-12.62	436	-15.34
4.	1782	1372	-23.01	1246	-30.08	1401	-21.38	1247	-30.02
5.	1263	1067	-15.52	947	-25.02	1054	-16.55	937	-25.82
6.	565	629	+11.33	562	- 0.53	534	- 5.49	497	-12.03
7.	1802	1370	-23.97	1218	-32.41	1357	-24.69	1217	-32.46
Mean Error			-13.37		-22.60		-19.23		-26.20
Standard Deviation			21.50		28.08		22.31		29.72

TABLE 4

CORRECTION FACTORS FOR NITROGEN CONTENT

(COOK-INLET BASIN CRUDE OILS)

	N_2 Correction (C_{N_2})	
SAMPLE	Jacobson[9]	Glaso[8]
1.	1.418	1.244
2.	1.280	1.172
3.	1.129	1.083
4.	1.350	1.210
5.	1.265	1.168
6.	1.103	1.079
7.	1.398	1.236

TABLE 5

COOK-INLET BASIN CRUDE OILS PREDICTED BUBBLE-POINT PRESSURES

-Corrected for Nitrogen Content-

		Bubble-Point Pressure Corrected with Glaso[8] Correlation								Bubble-Point Pressure Corrected with Jacobson[9] Correlation							
		Vazquez-Beggs[21]		Standing[19]		Glaso[8]		Lasater[13]		Vazquez-Beggs[21]		Standing[19]		Glaso[8]		Lasater[13]	
SAMPLE	Experimental Bubble-Point Pressure (psia)	P_b	%Error	P_b	%Error	P_b	%Err.	P_b	%Err.	P_b	%Err.	P_b	%Err.	P_b	%Err.	P_b	%Error
1.	1637	1468	-10.3	1314	-19.7	1470	-10.2	1317	-19.6	1673	+ 2.2	1504	- 8.1	1669	+ 1.9	1501	- 8.3
2.	1159	1064	- 8.2	955	-17.6	1011	-12.8	918	-20.8	1162	+ 0.3	1043	-10.0	1100	- 5.1	1003	-13.5
3.	515	598	+16.1	529	+ 2.7	488	- 5.2	473	- 8.2	623	+21.0	551	+ 7.0	508	- 1.4	493	- 4.3
4.	1782	1661	- 6.8	1507	-15.4	1695	- 4.9	1509	-15.3	1851	+ 3.9	1582	-11.2	1891	+ 6.1	1684	- 5.5
5.	1263	1256	- 0.6	1138	- 9.9	1229	- 2.7	1095	-13.3	1360	+ 7.7	1232	- 2.5	1333	+ 5.5	1186	- 6.1
6.	565	679	+20.2	606	+ 7.3	576	+ 2.0	537	- 5.0	693	+22.7	620	+ 9.7	589	+ 4.3	549	- 2.8
7.	1802	1694	- 6.0	1505	-16.5	1645	- 8.7	1504	-16.5	1914	+ 6.2	1704	- 5.4	1923	+ 6.7	1701	- 5.6
Mean Error			+ 0.64		- 9.88		- 6.08		-14.09		+ 9.12		- 2.93		+ 2.59		- 6.58
Standard Deviation			12.40		15.09		8.22		16.28		13.36		8.86		5.21		7.91

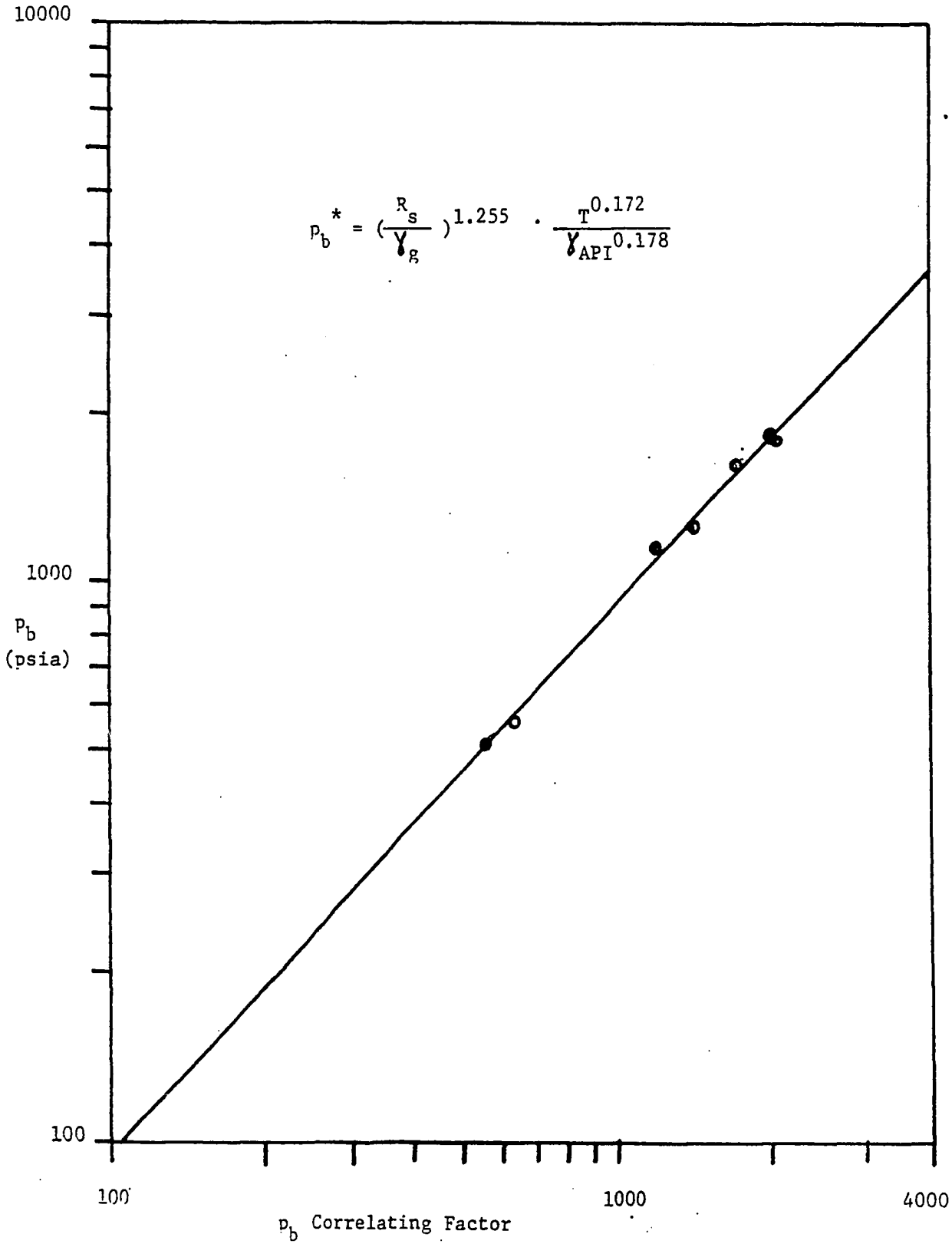

FIG. 11 : p_b vs. p_b CORRELATING FACTOR DEVELOPED FOR COOK INLET BASIN HYDROCARBON SYSTEMS

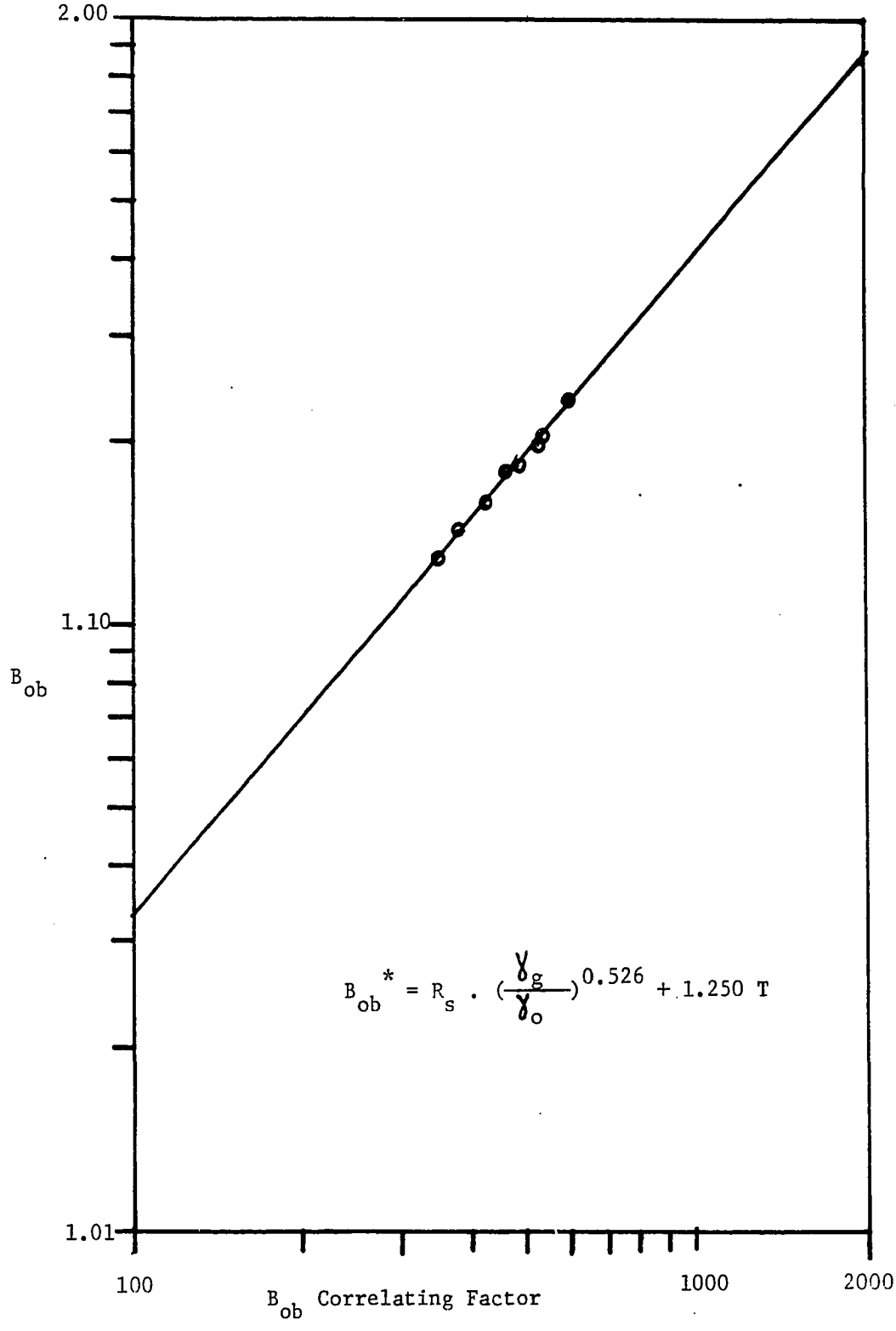

FIG. 12: B_{ob} VS. B_{ob} CORRELATING FACTOR DEVELOPED FOR COOK - INLET BASIN HYDROCARBON SYSTEMS

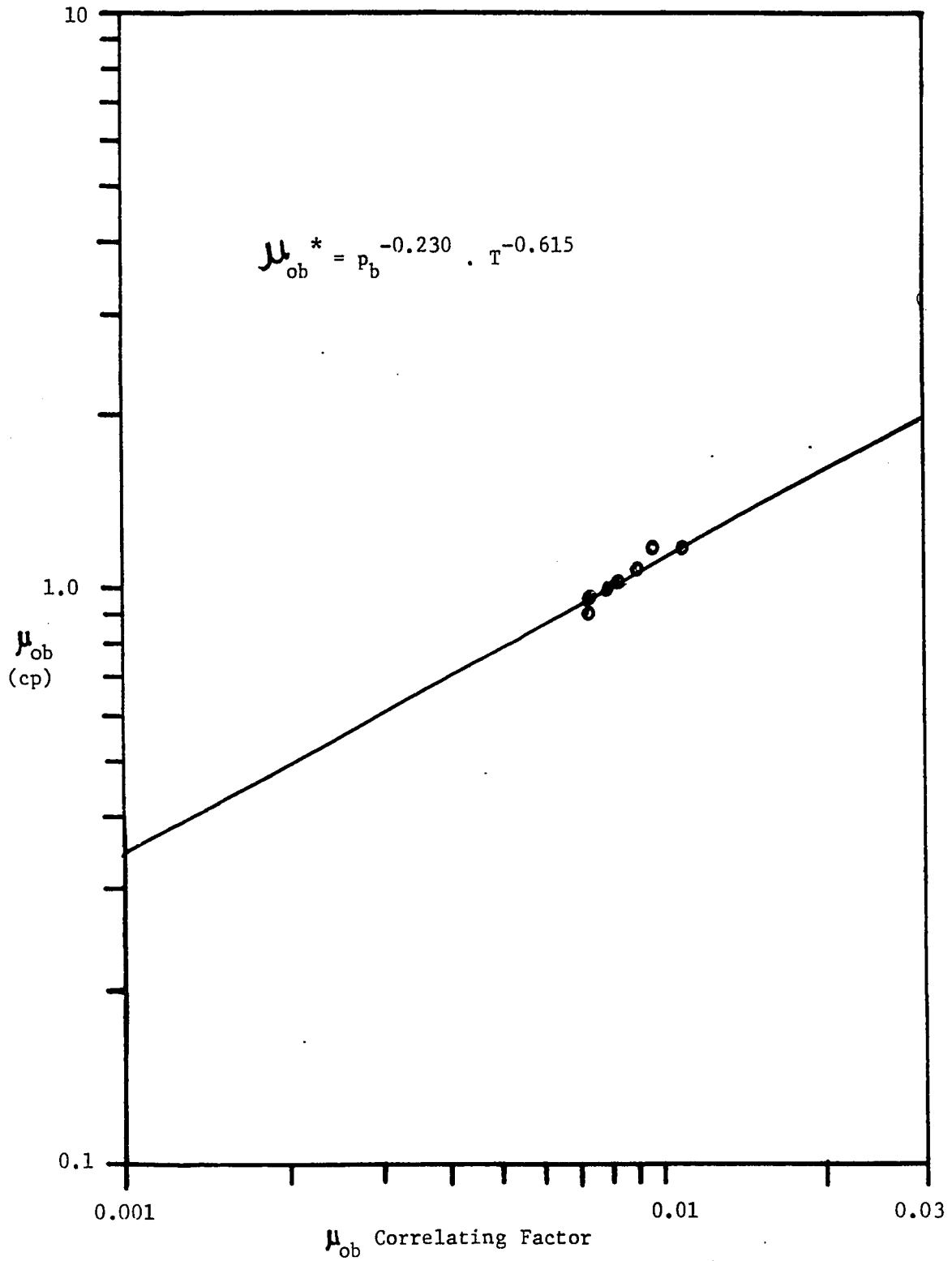

FIG. 13: μ_{ob} VS. μ_{ob} CORRELATING FACTOR DEVELOPED FOR COOK INLET BASIN HYDROCARBON SYSTEMS

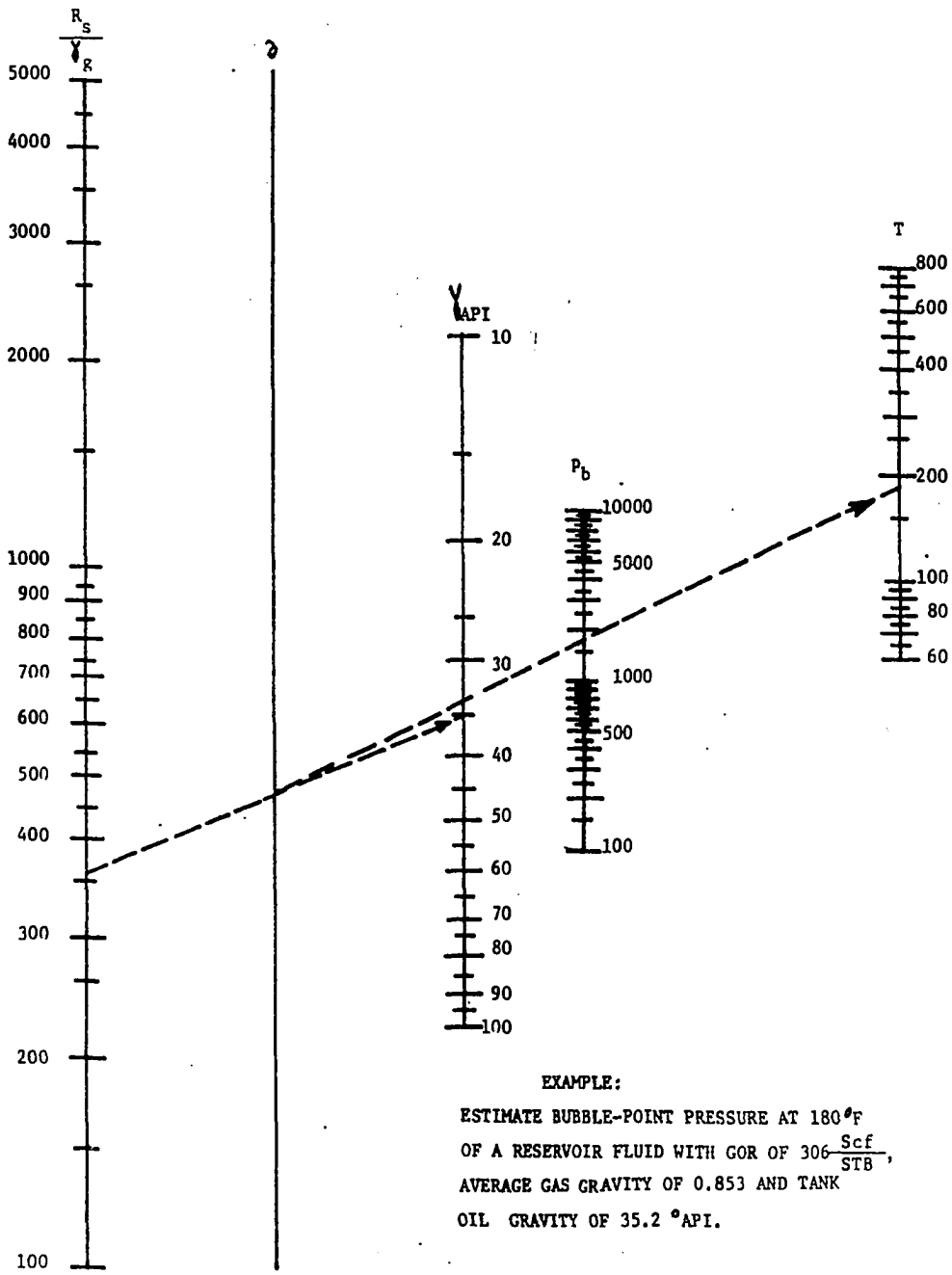

FIG. 14: BUBBLE-POINT PRESSURE CORRELATION FOR COOK INLET BASIN, ALASKA HYDROCARBON SYSTEMS

TABLE 6

PREDICTED BUBBLE-POINT PRESSURES USING THE NEW COOK-INLET BASIN CORRELATION

SAMPLE	Experimental Bubble-Point Pressure (psia)	Predicted Bubble-Point Pressure P_b	% Error
1.	1637	1548	-5.44
2.	1159	1083	-6.56
3.	515	536	+4.08
4.	1782	1858	+4.26
5.	1263	1294	+2.45
6.	565	600	+6.19
7.	1802	1812	+0.55
Mean Error			+0.79
Standard Deviation			5.03

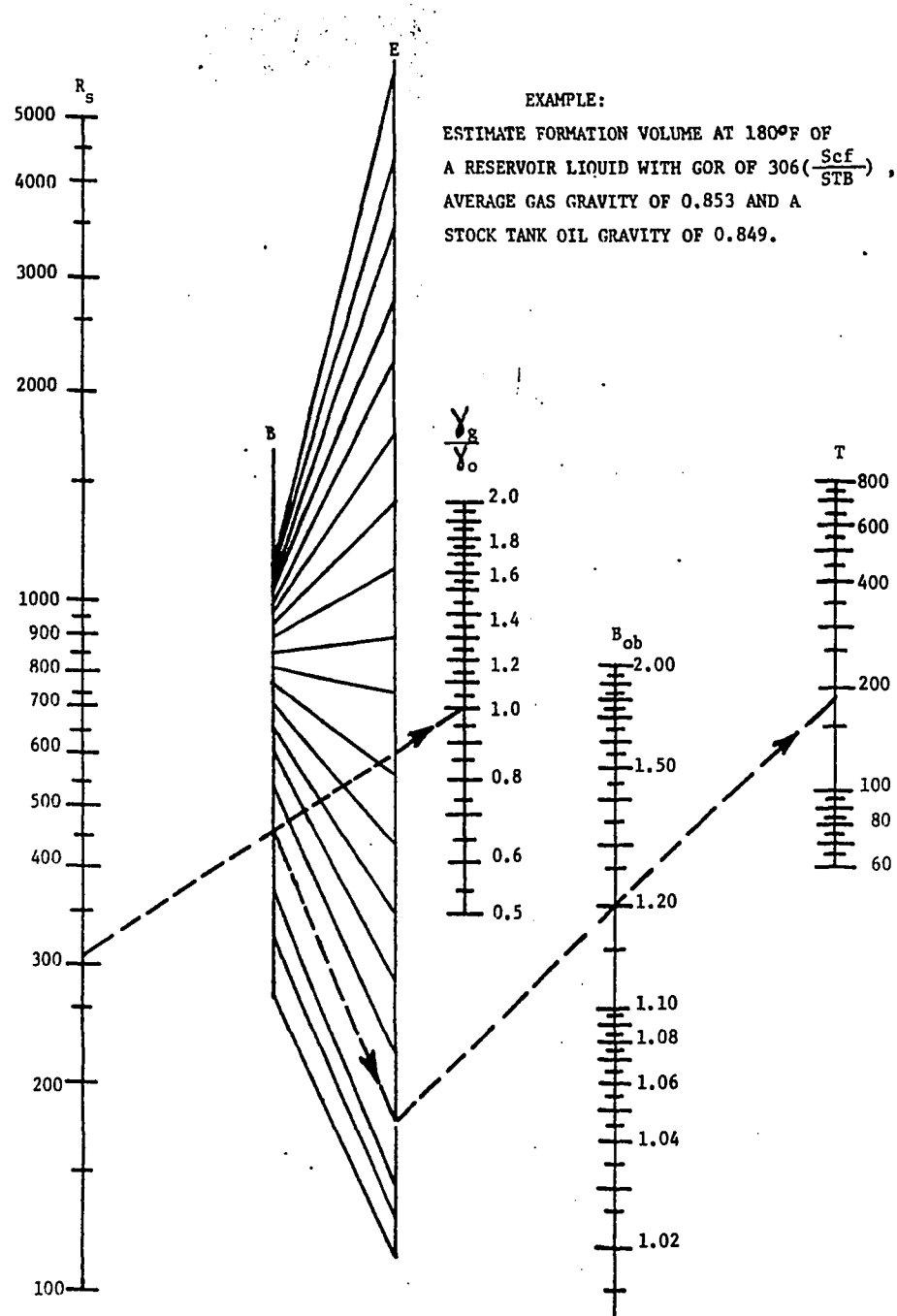

FIG. 15: BUBBLE-POINT OIL FORMATION VOLUME FACTORS CORRELATION FOR COOK INLET BASIN, ALASKA HYDROCARBON SYSTEMS

TABLE 7

EXPERIMENTAL AND PREDICTED OIL FORMATION VOLUME FACTOR

FOR COOK-INLET BASIN CRUDE OILS

		Predicted Oil Formation Factor at Bubble-Point							
		Standing[19]		Vazquez-Beggs[21]		Glaso[8]		New CIB	
SAMPLE	Experimental B_{ob} (Res.Bbl/STB)	B_{ob}	%Error	B_{ob}	%Error	B_{ob}	%Error	B_{ob}	%Error
1.	1.185	1.178	-0.591	1.174	-0.928	1.155	-2.532	1.186	+0.084
2.	1.160	1.148	-1.034	1.142	-1.552	1.125	-3.017	1.161	+0.086
3.	1.129	1.111	-1.594	1.098	-2.746	1.089	-3.543	1.130	+0.089
4.	1.199	1.200	+0.083	1.198	-0.083	1.173	-2.168	1.203	+0.334
5.	1.179	1.167	-1.018	1.163	-1.357	1.140	-3.308	1.178	-0.085
6.	1.144	1.125	-1.661	1.110	-2.972	1.098	-4.021	1.141	-0.262
7.	1.205	1.204	-0.083	1.200	-0.415	1.117	-7.303	1.207	+0.166
Mean Error			-0.843		-1.436		-3.699		+0.059
Standard Deviation			1.138		1.900		4.344		0.199

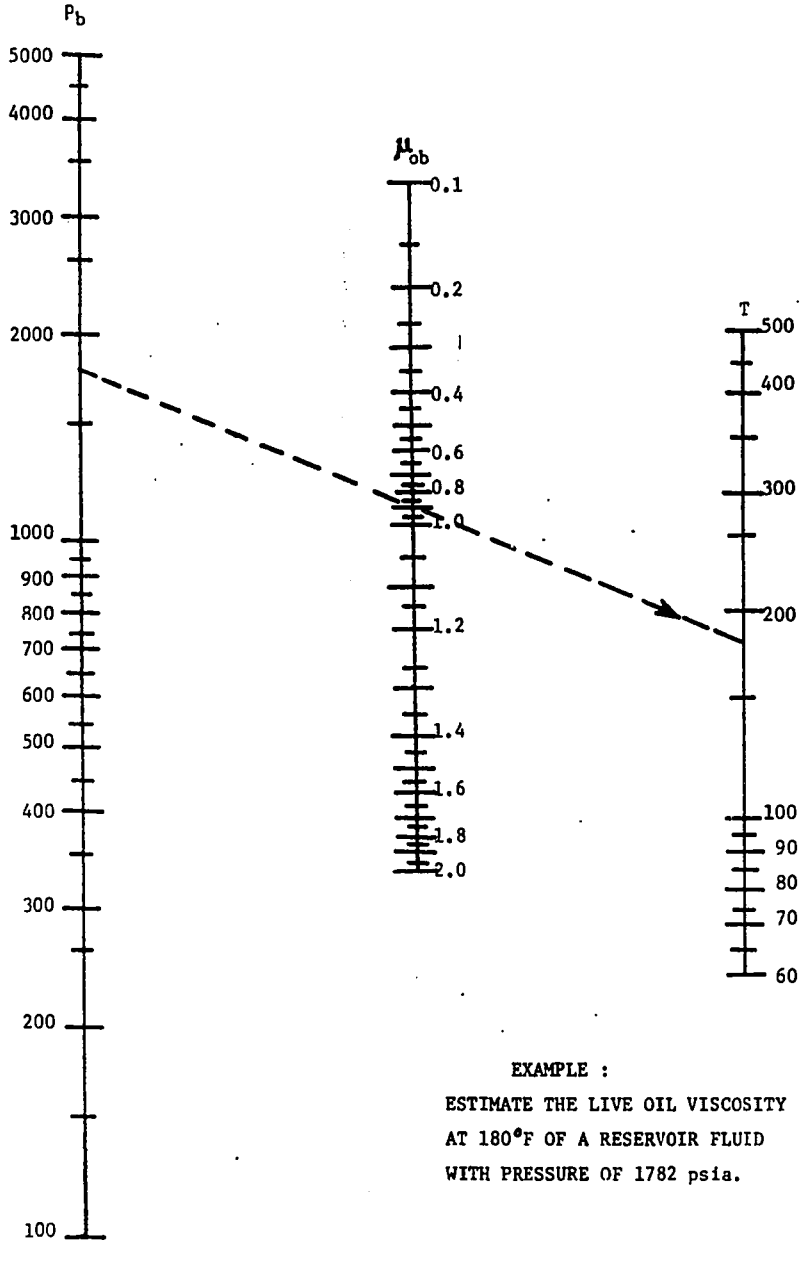

FIG. 16: OIL VISCOSITY CORRELATION FOR COOK INLET BASIN, ALASKA HYDROCARBON SYSTEMS

TABLE 8

EXPERIMENTAL AND PREDICTED OIL VISCOSITY FOR COOK-INLET BASIN CRUDE OILS

	Live Oil Viscosity at the Bubble-Point						Dead Oil Viscosity					
		Beggs & Robinson[2]		Beal[1]		New CIB		Beggs & Robinson[2]		Beal[1]		New CIB
SAMPLE	Experimental μ_{ob} (cp)	μ_{ob}	%Error	μ_{ob}	%Error	μ_{ob} %Error	Experimental μ_{od} (cp)	μ_{od}	%Error	μ_{od}	%Error	μ_{od} %Error
1.	1.05	1.09	+3.81	1.00	-4.76	1.07 +1.90	2.48	3.10	+25.00	2.65	+6.85	2.29 -7.66
2.	1.13	1.23	+8.85	1.22	+7.96	1.16 +2.65	2.48	3.01	+21.37	2.60	+4.84	2.29 -7.66
3.	1.32	1.58	+19.7	1.45	+9.85	1.37 +3.79	2.48	3.12	+25.81	2.65	+6.85	2.29 -7.66
4.	0.90	0.82	-8.89	0.84	-6.67	0.93 -3.33	2.10	2.15	+2.38	1.70	-19.0	2.17 +3.33
5.	1.00	0.95	-5.00	0.90	-10.0	1.02 +2.00	2.10	2.20	+4.76	1.75	-16.7	2.17 +3.33
6.	1.33	1.24	-6.77	1.30	-2.26	1.23 -7.52	2.10	2.31	+10.0	2.05	-2.38	2.17 +3.33
7.	0.96	0.81	-15.6	0.80	-16.7	0.93 -3.12	2.05	2.12	+3.30	1.60	-21.9	2.17 +5.85
Mean Error			-0.70		-3.22	-0.52			+13.23		-5.93	-1.02
Standard Deviation			12.08		10.09	4.21			17.73		14.41	6.37

TABLE 9

PVT PROPERTIES OF ALASKAN NORTH SLOPE CRUDE OILS

SAMPLE	T_s (°F)	p_s (psia)	γ_g	γ_{API} (°API)	$Y_{N_2+CO_2}$ (Res. Fluid) (%)	T (°F)	R_s (Scf/STB)	p_b (psia)	B_{ob} (Res.Bbl/STB)	μ_{ob} (cp)
1.	97	120	0.717	26.6	0.61	145	548	2900	1.265	1.58
2.	70	115	0.727	25.7	0.75	147	453	2615	1.219	1.96
3.	125	115	0.691	23.5	0.79	148	493	3045	1.223	2.55
4.	75	115	0.691	26.5	0.80	150	465	2980	1.224	2.28
5.	150	115	0.663	18.9	0.48	150	341	2480	1.167	9.80
6.	150	115	0.673	21.2	0.62	150	373	2585	1.176	4.00
7.	72	115	0.759	25.4	0.42	152	557	2965	1.270	1.62
8.	73	120	0.690	20.6	0.78	154	396	2840	1.202	4.84
9.	130	65	0.685	22.6	0.90	154	465	2990	1.216	2.52
10.	130	65	0.733	25.8	0.71	155	517	2830	1.266	1.54
11.	69	115	0.708	25.1	0.55	155	452	2770	1.214	1.85
12.	69	115	0.704	24.0	0.52	155	486	2967	1.243	1.82
13.	158	115	0.673	22.2	0.83	158	348	2485	1.175	3.10
14.	130	65	0.754	22.5	0.73	158	495	3010	1.255	2.30
15.	160	115	0.665	20.6	0.84	160	341	2535	1.171	4.87
16.	100	65	0.689	23.7	0.83	160	455	3095	1.225	2.02
17.	90	265	0.728	26.0	0.59	165	473	2550	1.232	1.47
18.	N/A	N/A	N/A	28.4	12.88	185	850	4310	1.399	0.69
19.	N/A	N/A	N/A	26.8	N/A	201	651	4507	1.325	1.06
20.	N/A	N/A	N/A	25.2	N/A	220	595	4102	1.307	1.34

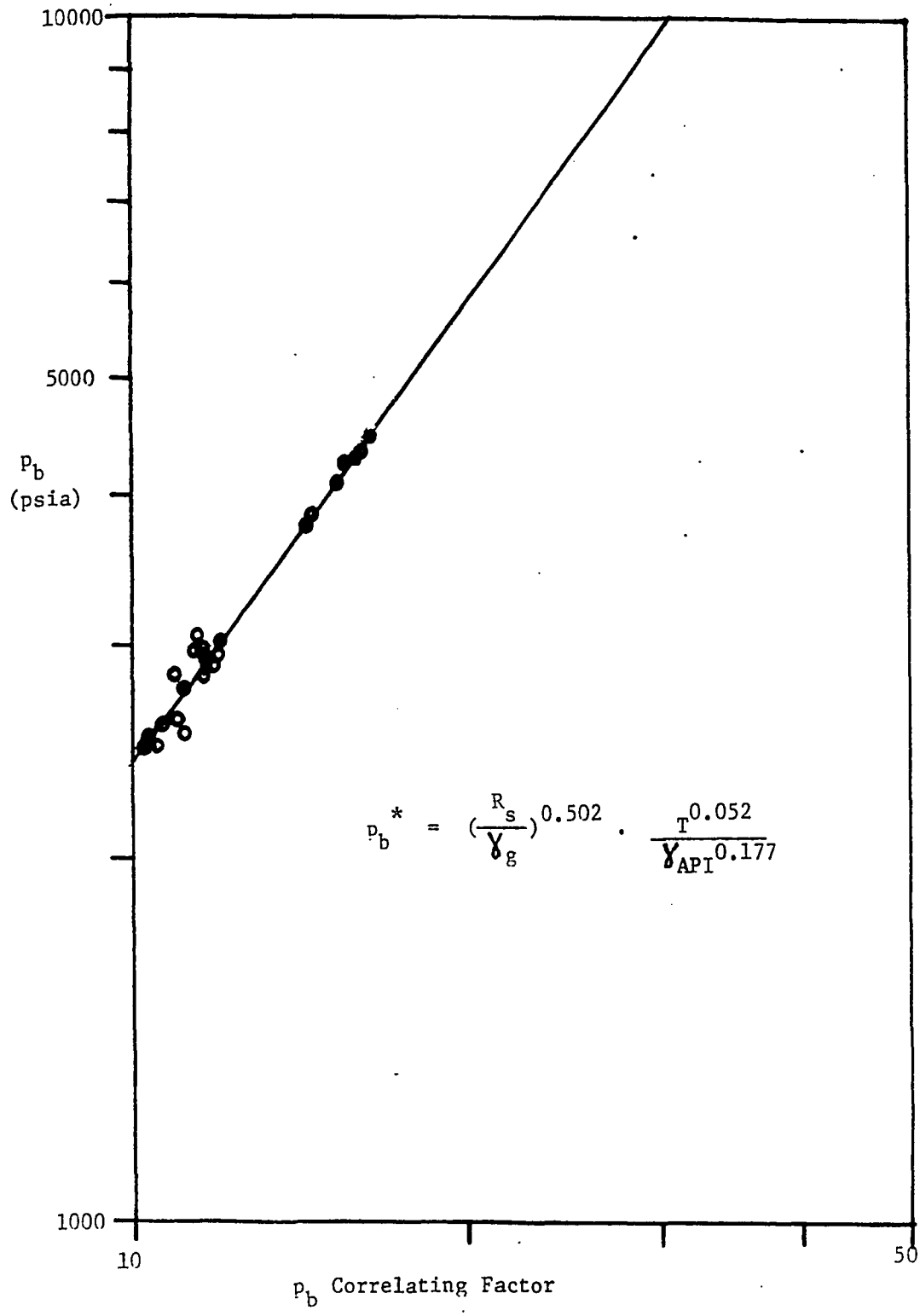

FIG. 17 : p_b VS. p_b CORRELATING FACTOR DEVELOPED FOR ALASKAN NORTH SLOPE HYDROCARBON SYSTEMS

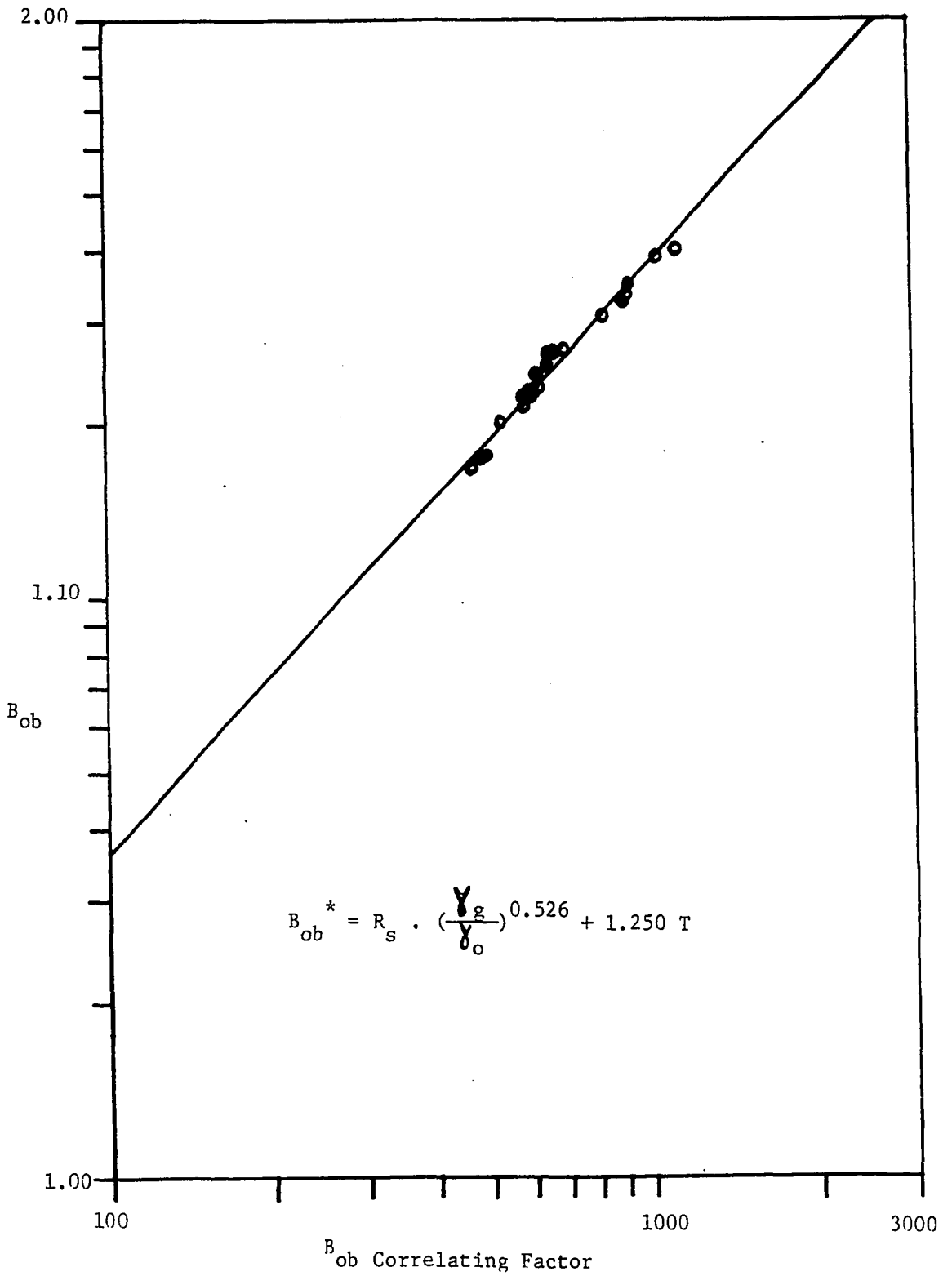

FIG. 18: B_{ob} vs. B_{ob} CORRELATING FACTOR DEVELOPED FOR ALASKAN NORTH SLOPE HYDROCARBON SYSTEMS

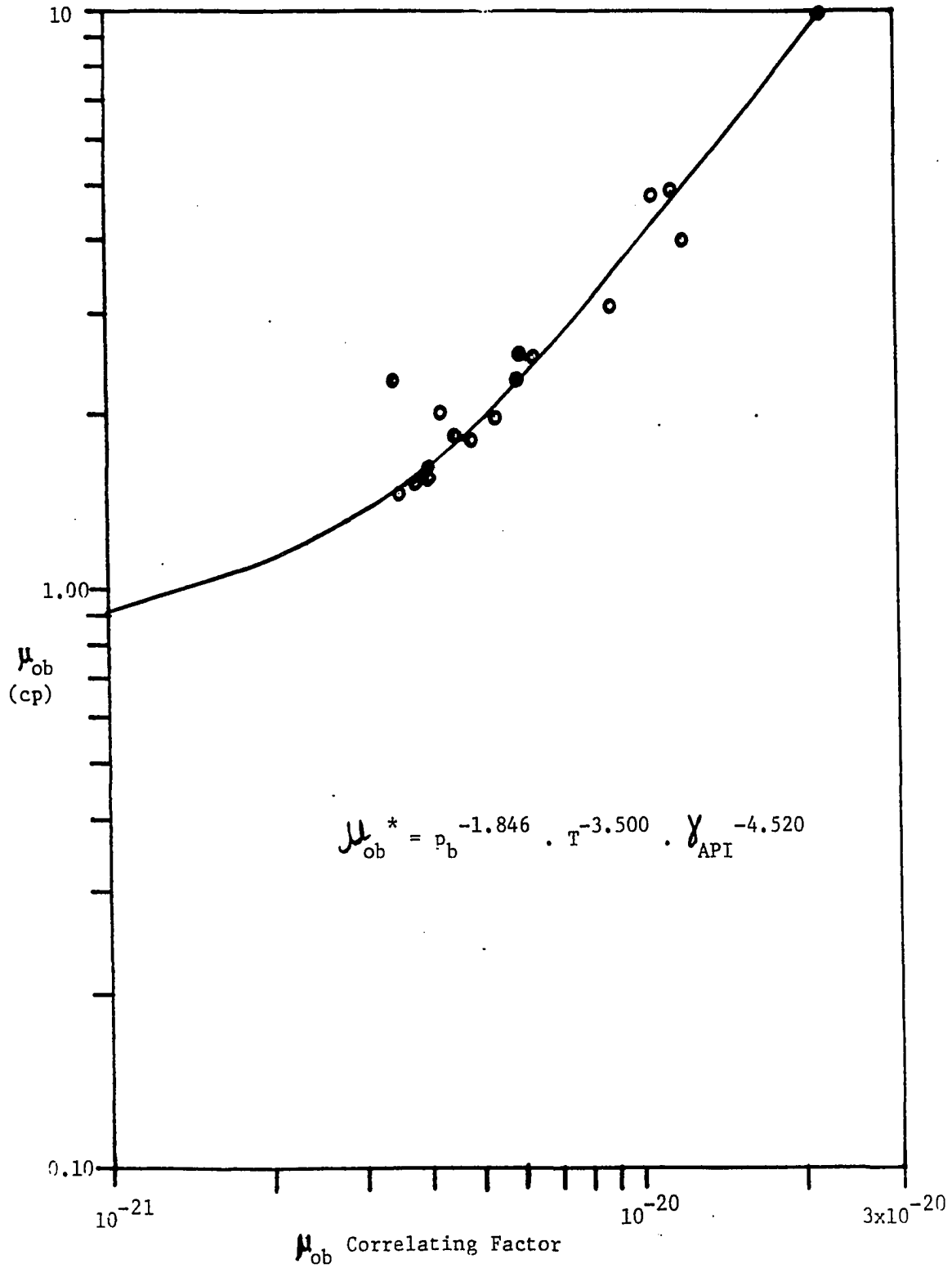

FIG. 19: μ_{ob} VS. μ_{ob} CORRELATING FACTOR DEVELOPED FOR ALASKAN NORTH SLOPE HYDROCARBON SYSTEMS

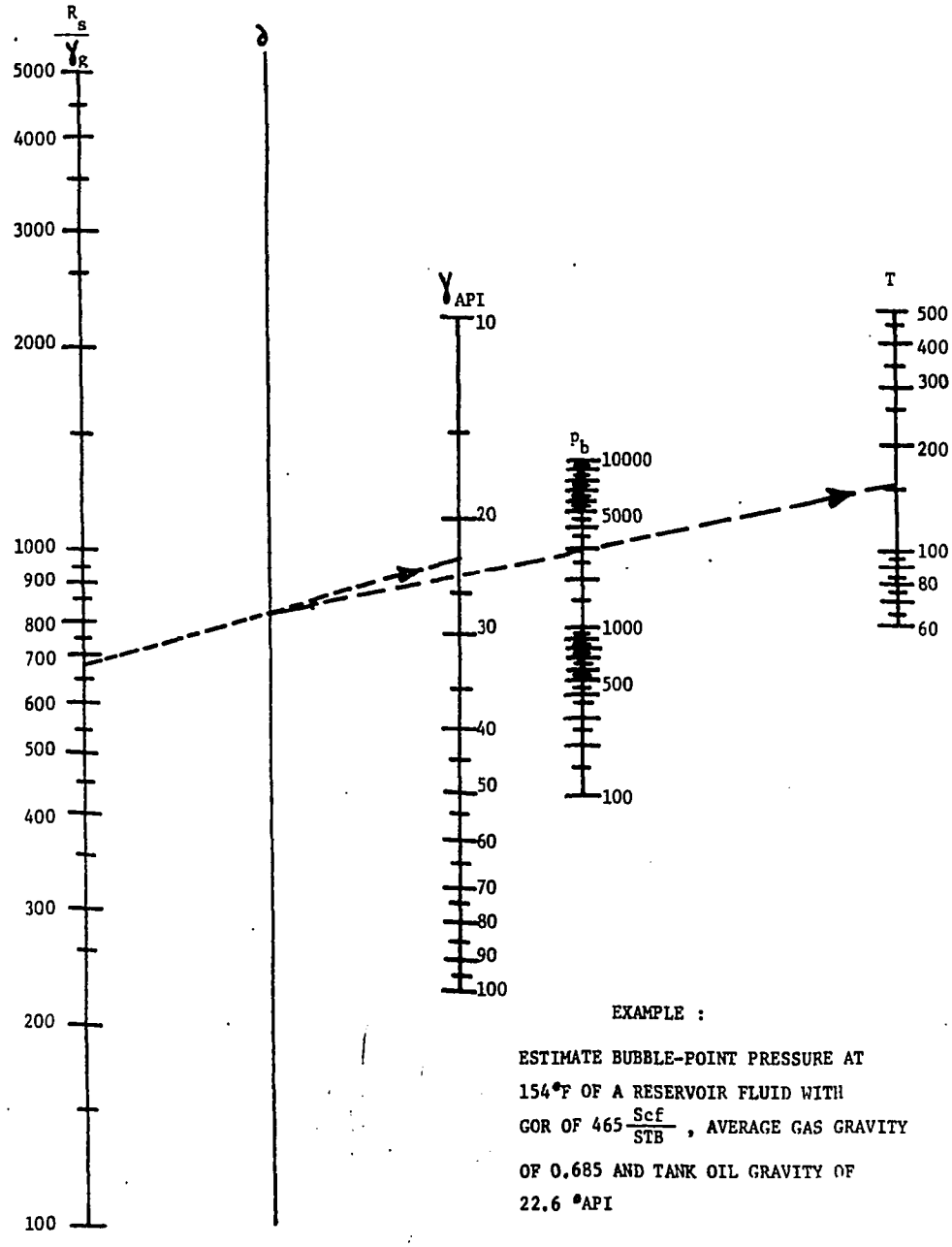

FIG. 20: BUBBLE-POINT PRESSURE CORRELATION FOR ALASKAN NORTH SLOPE HYDROCARBON SYSTEMS

TABLE 10

BUBBLE-POINT PRESSURES PREDICTED FROM PVT CORRELATIONS FOR ALASKAN NORTH SLOPE CRUDE OILS

SAMPLE	Experimental Bubble-Point Pressure (psia)	Predicted Bubble - Point Pressure									
		Vazquez-Beggs[21]		Standing[19]		Glaso[8]		Lasater[13]		New ANS	
		P_b	%Error	P_b	%Error	P_b	%Error	P_b	%Error	P_b	%Error
1.	2900	3188	+ 9.93	2723	- 6.10	3370	+16.21	2875	- 0.86	2947	+ 1.62
2.	2615	2755	+ 5.35	2441	- 6.65	3039	+16.21	2700	+ 3.25	2645	+ 1.03
3.	3045	3401	+10.47	2919	- 4.14	3706	+21.71	3000	- 1.48	2975	- 2.30
4.	2980	2880	- 3.36	2560	-14.09	3170	+ 6.38	2750	- 7.72	2762	- 7.32
5.	2480	3020	+21.77	2547	+ 2.70	3538	+42.66	2750	+10.89	2478	- 0.08
6.	2585	2959	+14.47	2537	- 1.86	2686	+ 3.91	2720	+ 5.22	2541	- 1.70
7.	2965	3264	+10.08	2855	- 3.71	3540	+19.39	3195	+ 7.76	2972	+ 0.24
8.	2840	3138	+10.49	2682	- 5.56	3570	+25.70	3150	+10.92	2625	- 7.57
9.	2990	3533	+18.16	2913	- 2.58	3725	+24.58	3210	+ 7.36	2891	- 3.31
10.	2830	3261	+15.23	2696	- 4.74	3391	+19.82	2915	+ 3.00	2874	+ 1.55
11.	2770	2920	+ 5.42	2577	- 6.97	3219	+16.21	2900	+ 4.69	2688	- 2.96
12.	2967	3272	+10.28	2841	- 4.25	3570	+20.32	2850	- 3.94	2880	- 2.93
13.	2485	2702	+ 8.73	2365	- 4.83	3074	+23.70	2560	+ 3.02	2373	- 4.51
14.	3010	3459	+14.92	2863	- 4.88	3659	+21.56	3000	- 0.33	2821	- 6.28
15.	2535	2857	+12.70	2472	- 2.49	4271	+68.48	2625	+ 3.55	2405	- 5.13
16.	3095	3306	+ 6.82	2790	- 9.86	3509	+13.38	2950	- 4.68	2793	- 9.76
17.	2550	2786	+ 9.26	2604	+ 2.12	3191	+25.14	2788	+ 9.33	2691	+ 5.53
Mean Error			+10.63		- 4.58		+22.67		+ 2.94		- 2.41
Standard Deviation			12.33		6.14		27.51		6.27		4.78

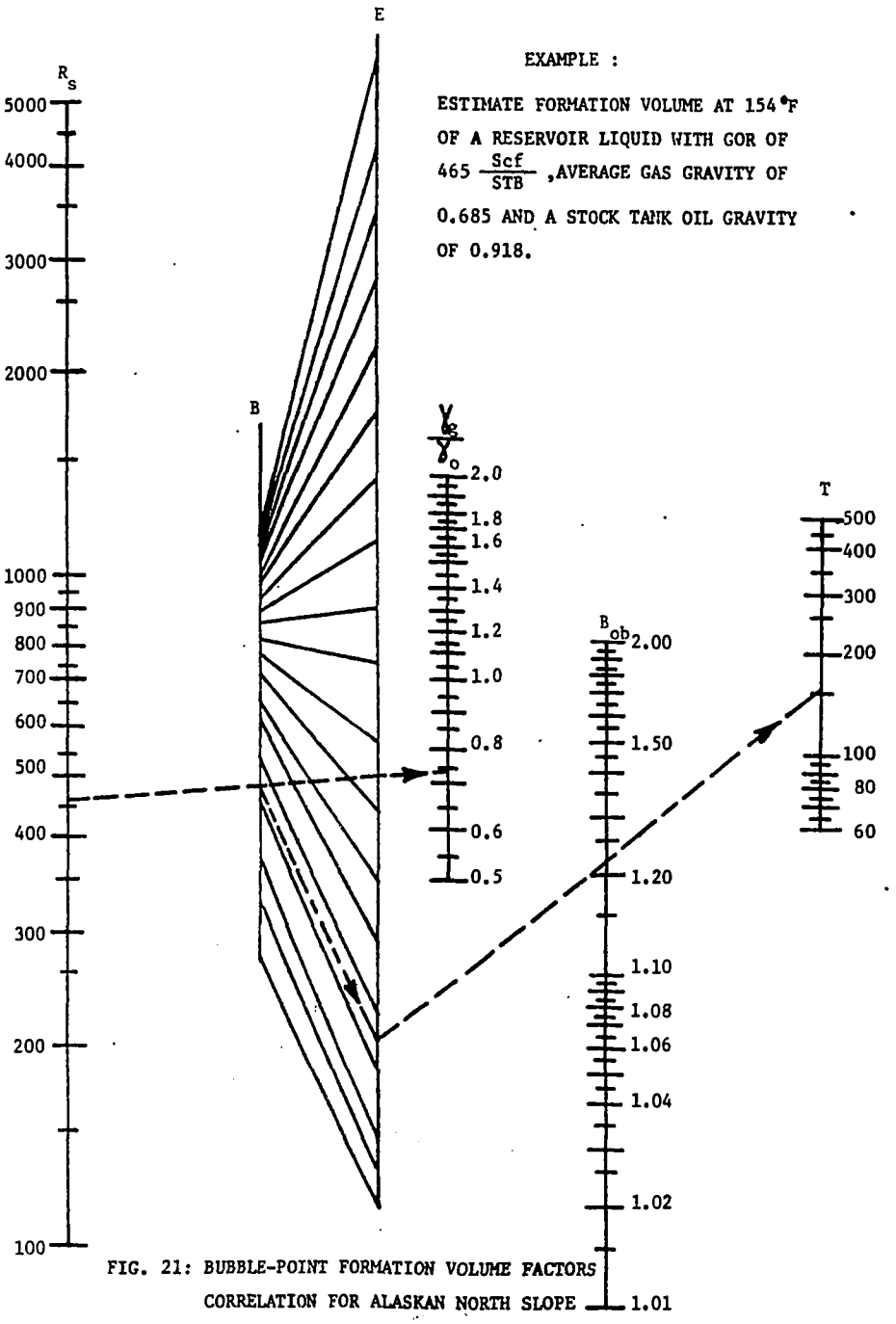

FIG. 21: BUBBLE-POINT FORMATION VOLUME FACTORS CORRELATION FOR ALASKAN NORTH SLOPE HYDROCARBON SYSTEMS

TABLE 11

EXPERIMENTAL AND PREDICTED OIL FORMATION VOLUME FACTOR AT BUBBLE-POINT FOR ALASKAN NORTH SLOPE CRUDE OILS

		Predicted Oil Formation Volume Factor at Bubble-Point							
		Vasquez-Beggs[21]		Standing[19]		Glaso[8]		New ANS	
SAMPLE	Experimental Oil Formation Volume Factor (Res.Bbl/STB)	B_{ob}	%Error	B_{ob}	%Error	B_{ob}	%Error	B_{ob}	%Error
1.	1.265	1.280	+1.186	1.272	+0.553	1.251	-1.107	1.249	-1.265
2.	1.219	1.240	+1.723	1.230	+0.902	1.207	-0.984	1.219	0.000
3.	1.223	1.256	+2.698	1.242	+1.541	1.218	-0.409	1.227	+0.327
4.	1.224	1.249	+2.043	1.233	+0.735	1.209	-1.226	1.221	-0.245
5.	1.167	1.189	+1.885	1.171	+0.343	1.146	-1.800	1.175	+0.686
6.	1.176	1.205	+2.466	1.187	+0.935	1.162	-1.191	1.183	+0.595
7.	1.270	1.283	+1.024	1.288	+1.417	1.266	-0.315	1.261	-0.709
8.	1.202	1.214	+0.998	1.201	-0.083	1.176	-2.163	1.197	-0.416
9.	1.216	1.247	+2.486	1.232	+1.316	1.208	-0.658	1.220	+0.329
10.	1.266	1.270	+0.316	1.266	0.000	1.243	-1.817	1.245	-1.659
11.	1.214	1.243	+2.388	1.231	+1.400	1.207	-0.577	1.216	+0.165
12.	1.243	1.256	+1.046	1.246	+0.241	1.222	-1.690	1.230	-1.046
13.	1.175	1.199	+2.043	1.181	+0.511	1.156	-1.617	1.183	+0.681
14.	1.255	1.258	+0.239	1.259	+0.319	1.235	-1.594	1.240	-1.195
15.	1.171	1.195	+2.050	1.178	+0.598	1.152	-1.623	1.180	+0.769
16.	1.225	1.246	+1.714	1.232	+0.571	1.207	-1.469	1.220	-0.408
17.	1.232	1.253	+1.705	1.252	+1.623	1.227	-0.406	1.235	+0.244
Mean Error			+1.648		+0.760		-1.214		-0.185
Standard Deviation			1.852		0.951		1.377		0.789

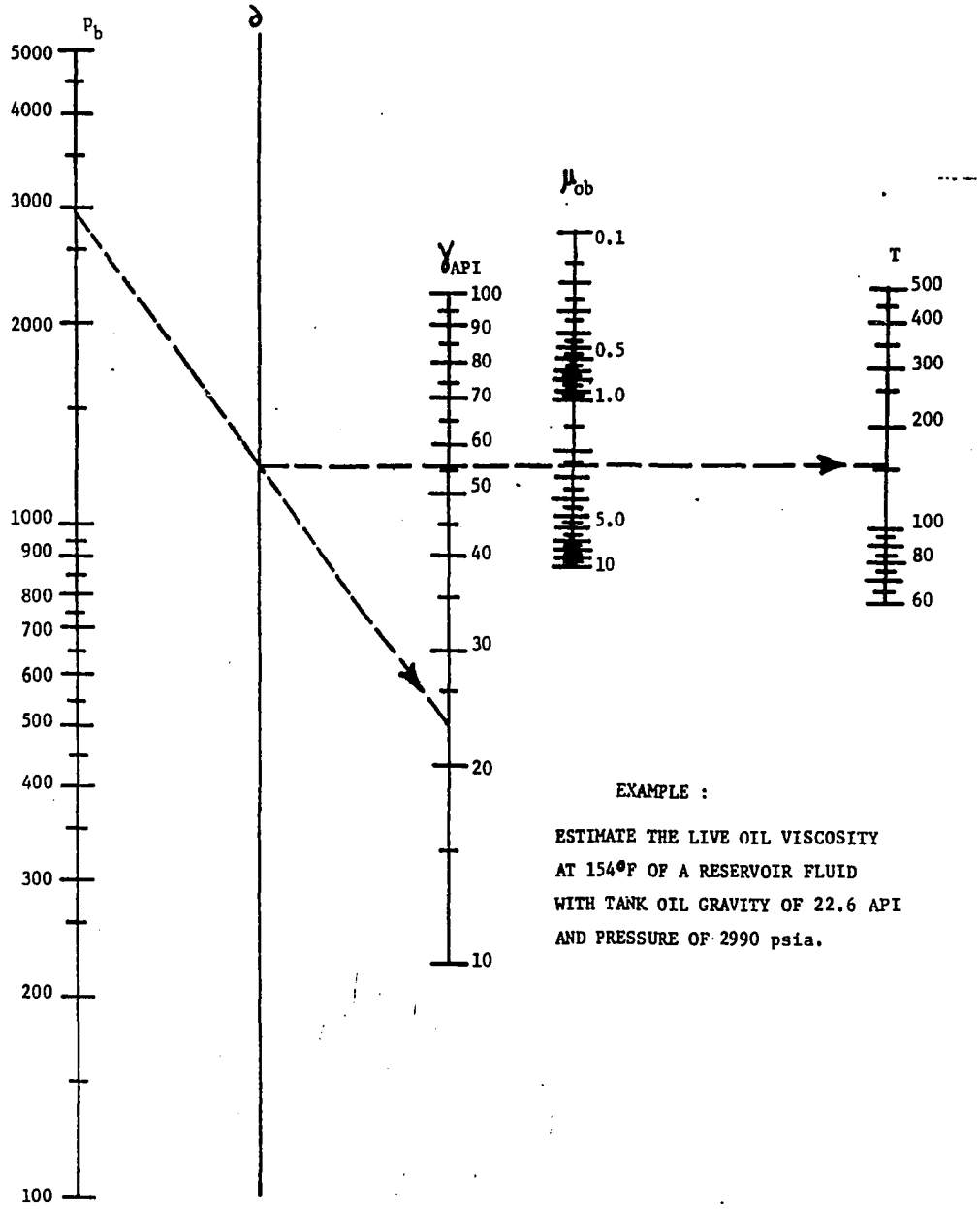

FIG. 22: OIL VISCOSITY CORRELATION FOR ALASKAN NORTH SLOPE HYDROCARBON SYSTEMS

TABLE 12

EXPERIMENTAL AND PREDICTED LIVE OIL VISCOSITY FOR ALASKAN NORTH SLOPE CRUDE OILS

SAMPLE	Experimental Live Oil Viscosity (cp)	Predicted Live Oil Viscosity at Bubble - Point					
		Beggs & Robinson[2]		Beal[1]		New ANS	
		μ_{ob}	%Error	μ_{ob}	%Error	μ_{ob}	%Error
1.	1.58	1.32	-16.46	1.90	+20.25	1.67	+5.70
2.	1.96	1.59	-18.88	2.40	+18.33	1.95	-0.51
3.	2.55	1.73	-32.16	2.60	+ 1.96	2.08	-18.43
4.	2.28	1.42	-37.72	2.10	- 7.89	1.57	-31.14
5.	9.80	3.43	-65.00	7.50	-23.47	12.86	+31.22
6.	4.00	2.56	-36.00	4.30	+ 7.50	4.21	+ 5.25
7.	1.62	1.30	-19.75	2.00	+23.46	1.67	+ 2.99
8.	4.84	2.42	-50.00	5.40	+11.57	3.54	-26.86
9.	2.52	1.80	-28.57	2.90	+15.08	2.19	-13.09
10.	1.54	1.30	-15.58	1.80	+16.88	1.64	+ 6.49
11.	1.85	1.51	-18.38	2.40	+29.73	1.74	- 5.95
12.	1.82	1.55	-14.84	2.50	+37.36	1.83	+0.55
13.	3.10	2.22	-28.39	4.10	+32.26	2.90	- 6.45
14.	2.30	1.64	-28.70	2.80	+21.74	2.06	-10.43
15.	4.87	2.54	-47.84	5.40	+10.88	3.89	-20.12
16.	2.02	1.57	-22.28	2.60	+28.71	1.72	-14.85
17.	1.47	1.23	-16.33	2.80	+90.48	1.59	+ 8.16
Mean Error			-29.23		+19.70		- 5.14
Standard Deviation			33.35		31.16		16.14

CHAPTER V

DIMENSIONLESS RESERVOIR FLUID BEHAVIOR OF ALASKAN CRUDES

INTRODUCTION

The purpose of this chapter is to present relationships that would facilitate the analysis of depletion-drive oil reservoirs for which no PVT analysis is available. The developed relationships provide guidelines for selection of a representative PVT sample for a similar oil and similar reservoir conditions. It is also possible to use them directly to estimate solution gas-oil ratios, formation volume factors and live oil viscosities at any stage of depletion, provided the oil in question can be considered average.

To achieve these objectives, comparisons of reservoir fluid behavior of crude oils from Cook Inlet Basin and Alaskan North Slope reservoirs, was made by reducing the available PVT data from these fields to sets of dimensionless graphs. These developed relationships are not intended as a substitute for laboratory PVT analysis, should they be available. They are designed to be used with the newly developed Alaskan correlations (Chapter 4) and reservoir information for determining bubble-point pressure, bubble-point solution gas-oil ratio, bubble-point oil formation volume factor, bubble-point live oil viscosity, reservoir temperature, and for prediction of all the above mention reservoir properties below the bubble-point and at

reservoir temperature. The correlations were made from differential liberation data, which were converted to flash data for this particular study. The correlations developed are presented in form of equations and graphs.

PROCEDURES

Using the available PVT reports from Alaskan fields, sets of dimensionless ratios were calculated. These ratios are dimensionless pressure, dimensionless solution gas-oil ratio, dimensionless formation volume factor and dimensionless live oil viscosity. It was possible to do this by converting the differential liberation data to flash data.

The differential process is thought to represent most closely the situation which exists in the reservoir. Free gas evolved from solution when pressure falls below bubble-point. This is because the free gas has a much larger mobility than the oil and so it is produced more readily. This resembles the differential process. Once in wellbore, the fluids undergo a flash transition from reservoir conditions to separator conditions, and again to stock tank conditions. It is necessary to convert the differential data to flash data. The flash data is converted from the differential data using the following equations:

$$B_{of} = B_{od} \left(B_{ofb} / B_{odb}\right) \qquad (32)$$

$$R_{sf} = R_{sfb} - \left(R_{sdb} - R_{sd}\right) \left(B_{ofb}/B_{odb}\right) \qquad (33)$$

The dimensionsless pressure is defined as pressure divided by bubble-point pressure.

$$P_D = P/P_b \qquad (34)$$

The dimensionless solution gas-oil ratio is defined as the solution gas-oil ratio at a pressure divided by the initial (bubble-point) solution gas-oil ratio.

$$R_{sD} = R_s/R_{sb} \qquad (35)$$

The dimensionless formation volume factor is defined as the shrinkage to a pressure below the bubble-point divided by total shrinkage from the bubble point to atmospheric pressure.

$$B_{oD} = (B_{ob} - B_o)/(B_{ob} - B_{oa}) \qquad (36)$$

The dimensionless live oil viscosity is defined as the live oil viscosity at a pressure below the bubble-point divided by the live oil viscosity at bubble-point.

$$\mu_{oD} = \mu_o / \mu_{ob} \qquad (37)$$

RESULTS AND DISCUSSION

Example of the data used in developing Figures 23 to 25, is shown in Table 13. The reservoir fluid values at bubble-point are as shown in Tables 2 and 9. In all the figures (Figs. 23 to 25), the "a" figures represent the data points and the "b" figures represent the developed correlating graphs.

Figure 23b is dimensionless solution gas-oil ratio vs. dimensionless pressure graphs for the Alaskan North Slope and the Cook Inlet Basin fields. Fig. 24b represents dimensionless oil formation volume factor vs. dimensionless pressure, while Fig. 25b represents dimensionless live oil viscosity vs. dimensionless pressure. From examination of the "a" part of the above mentioned figures, it is apparent that most of the points fall into a reasonably well defined trend, through which an average line has been drawn to represent the graphical correlation.

Cronquist[5], did a similar study on Gulf coast reservoir oils, but he failed to present his correlations in equation form. For this present study, the correlating equations are as stated below:

COOK-INLET BASIN

After applying regression analysis on the data of Figs. 23a, 24a and 25a, the following equations were developed to predict the dimensionless behavior of Cook-Inlet Basin reservoir fluid properties.

For the dimensionless solution gas-oil ratio, the relationship was:

$$R_{SD} = 1.0164\ P_b^{\ 0.4963} \qquad (38)$$

For the dimensionless formation volume factor at pressures below the bubble-point, the relationship was:

$$B_{OD} = 0.0771 - 0.1724\ \ln P_D \qquad (39)$$

For the dimensionless live-oil viscosity below the bubble-point, the relationship was:

$$\mu_{OD} = 0.9814 - 0.2299\ \ln P_D \qquad (40)$$

ALASKAN NORTH SLOPE

Regression analysis was also applied to Alaskan North Slope data of Figs. 23a, 24a, and 25a. The relationship developed for the dimensionless solution gas-oil ratio was as follows:

$$R_{SD} = 0.0243 + 0.9858\ P_D \qquad (41)$$

For the dimensionless formation volume factor below the bubble-point, the relationship was:

$$B_{OD} = 1.0124 - 1.0033\ P_D \qquad (42)$$

For the dimensionless live-oil viscosity below bubble point, the relationship was:

$$\mu_{OD} = 1.0083 - 0.6353\ \ln P_D \qquad (43)$$

The chief advantage of this type of correlation is two fold; first, it can be easily and rapidly used, and secondly, the basic data required are generally available or can be easily obtained. Most correlations of PVT properties require gas gravity, which is not always available.

EXAMPLE USE OF THE DIMENSIONLESS CORRELATIONS

As an example, consider a reservoir in Alaskan North Slope Field, with the following conditions:

Formation temperature	200°F
Initial Solution gas-oil ratio	730 Scf/STB
Initial Pressure	4,390 psia
Current Pressure	4,085 psia
Initial Formation Volume Factor	1.40 res.Bbl/STB.
Initial Oil Viscosity	0.81 cp
Oil Gravity	28°API

From geological and performance information it is known that the accumulation initially had a gas cap; therefore,

$$P_D = \frac{4,085}{4,390} = 0.931$$

From fig. 23b, at $P_D = 0.931$, $R_{SD} = 0.940$

Since, the initial solution gas-oil ratio was earlier determined to be 730 Scf/STB, therefore the predicted current solution ratio is thus (from Eq. 35):

$$R_s = R_{SD} \cdot R_{sb} = 0.940 \times 730 = 686 \text{ Scf/STB}$$

From Fig. 24b, at P_D= o.931, $B_{oD} = 0.03$. Since the value of the Boa is unknown, it can be estimated using Katz[11] correlation. Boa is estimated to be 1.060, and since the initial pressure was at bubble-point, $B_{ob} = 1.40$, same as given above. Which implies that the predicted current formation volume factor is determined as (from Eq. 36):

$$B_{OD} = 0.03 = \frac{1.40 - B_o}{1.40 - 1.060}$$

Thus,

$$B_o = 1.390 \text{ res.Bbl/STB}$$

From fig. 25b, at $P_b = 0.931$, $\mu_D = 1.02$.

Since the initial pressure was at bubble-point, the initial oil viscosity is the same as the oil viscosity at bubble-point, $\mu_{ob} = 0.81$ cp. Using Eq. 37, the current live oil viscosity is:

$$\mu_o = \mu_{oD} \cdot \mu_{ob} = 1.02 \times 0.81 = 0.826 \text{ cp.}$$

For Alaskan North Slope saturated crudes, these predictions can also be made using eqs. 41 to 43, and in the case of Cook Inlet Basin saturated crudes, Eqs. 38 to 40 apply.

TABLE 13

DIMENSIONLESS RESERVOIR FLUID BEHAVIOR EXAMPLE CALCULATION

Reservoir in Cook-Inlet Basin, Alaska:

Bubble-Point Pressure 1782psia
Bubble-Point Solution Gas-Oil Ratio 306Scf/STB
Reservoir Temperature ..... 180°F
Oil Gravity ..... 35.2°API

p	p_D	R_s	R_{sD}	B_o	B_{oD}	μ_o	μ_{oD}
1782	1.000	306	1.000	1.199	0.000	0.90	1.000
1615	0.905	284	0.942	1.191	0.040	0.92	1.022
1440	0.806	260	0.881	1.181	0.084	0.95	1.056
1263	0.706	237	0.820	1.172	0.129	1.00	1.111
1087	0.607	212	0.757	1.162	0.173	1.08	1.200
915	0.509	187	0.692	1.152	0.222	1.16	1.289
738	0.409	159	0.619	1.141	0.276	1.23	1.367
565	0.311	130	0.544	1.129	0.333	1.33	1.478
385	0.209	96	0.456	1.115	0.400	1.44	1.600
211	0.111	58	0.357	1.094	0.498	1.56	1.733
117	0.058	30	0.284	1.077	0.578	1.64	1.822

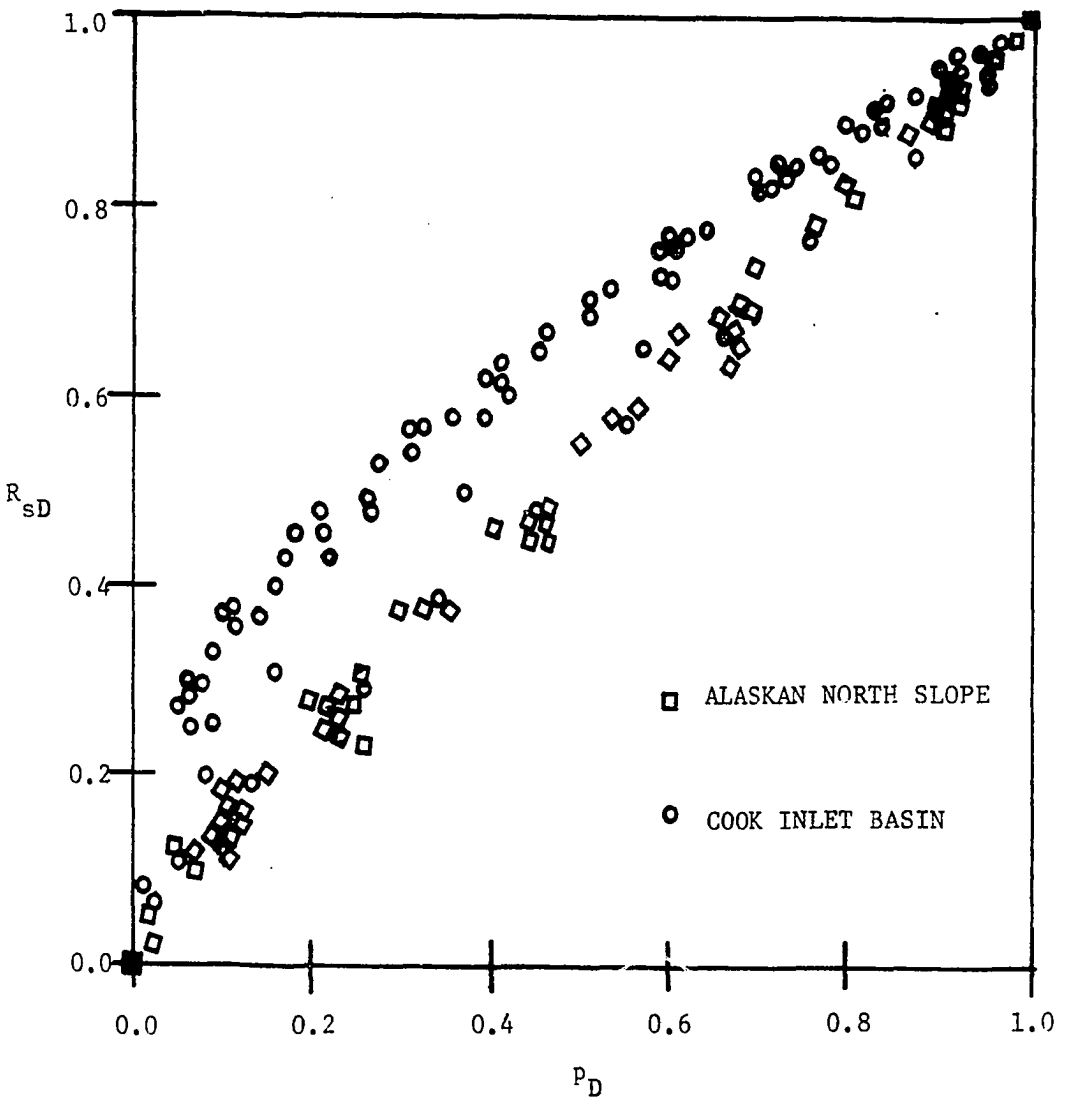

FIG. 23a : DIMENSIONLESS SOLUTION GAS - OIL RATIO VS. DIMENSIONLESS PRESSURE FOR SATURATED CRUDES

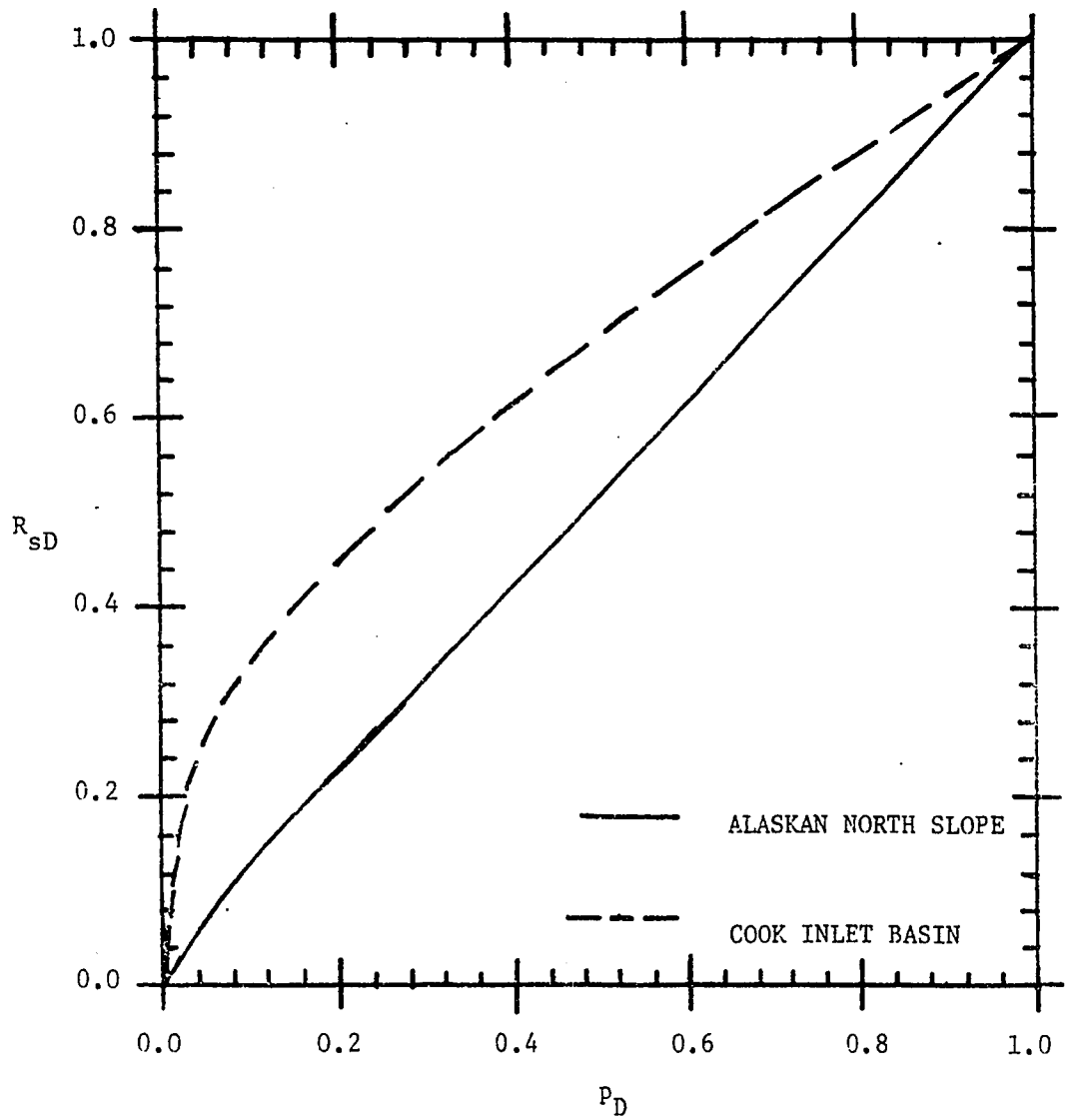

FIG. 23b : DIMENSIONLESS SOLUTION GAS - OIL RATIO VS. DIMENSIONLESS PRESSURE FOR SATURATED CRUDES

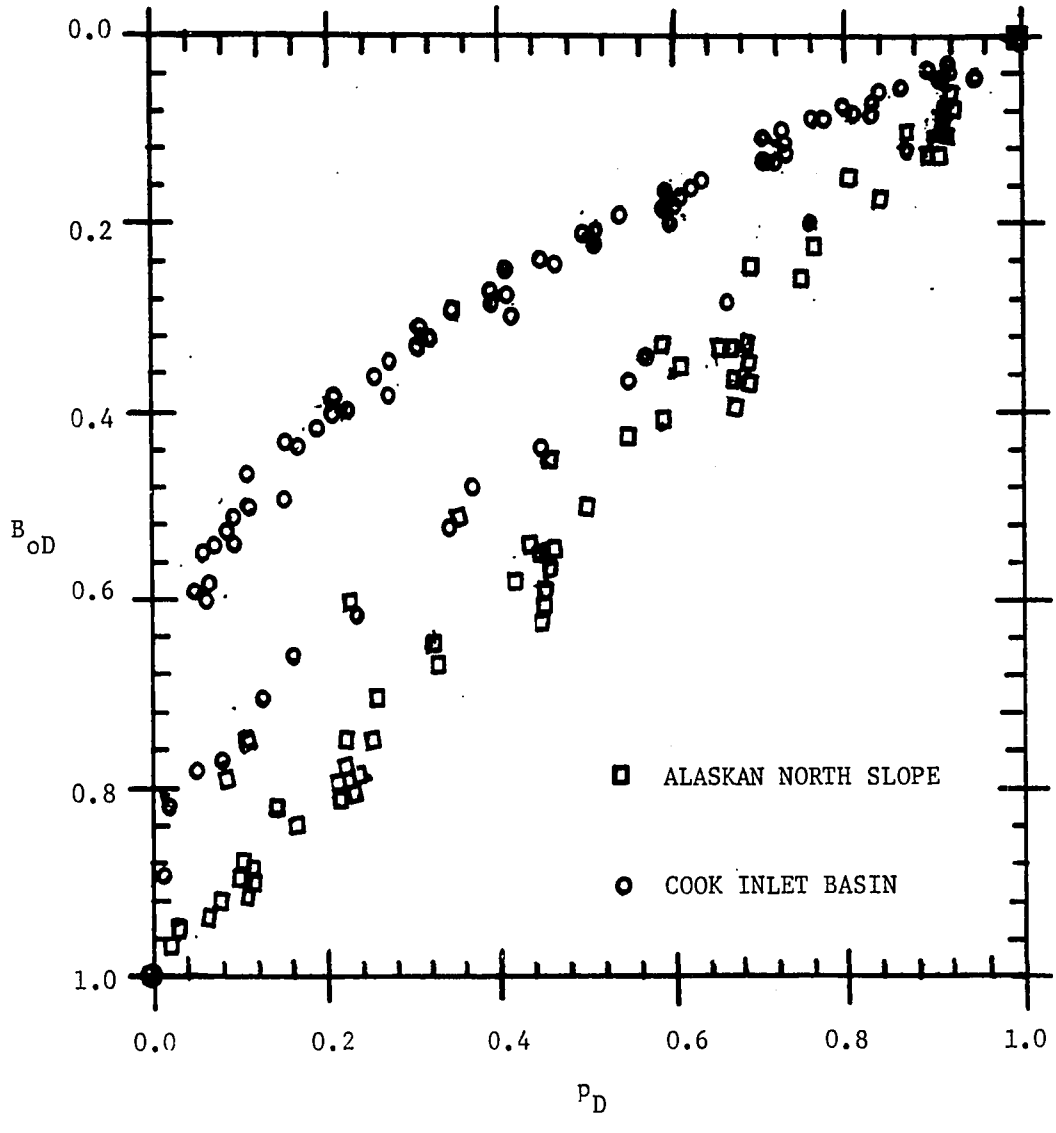

FIG. 24a : DIMENSIONLESS OIL FORMATION VOLUME FACTOR VS. DIMENSIONLESS PRESSURE FOR SATURATED CRUDES

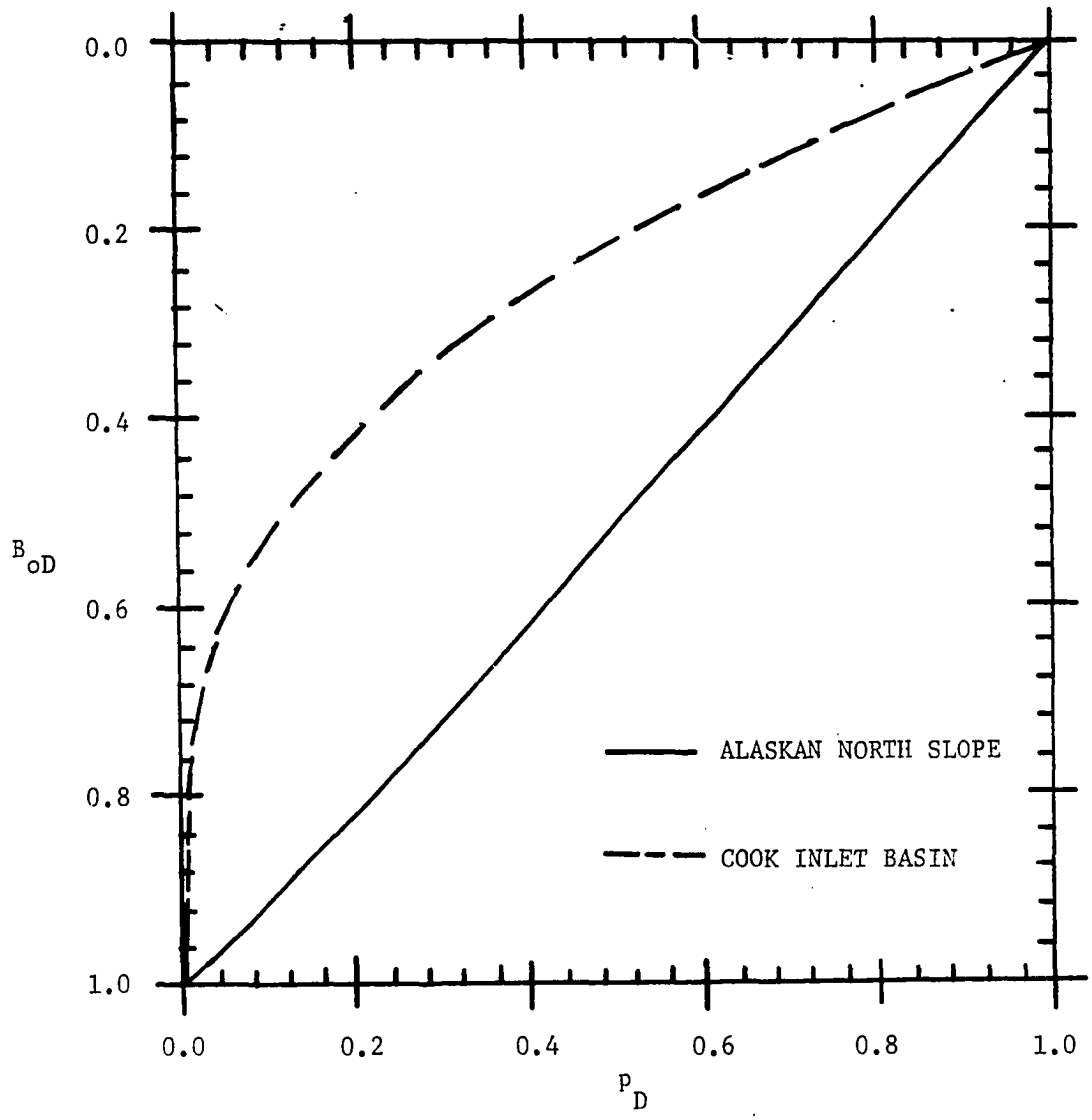

FIG. 24b : DIMENSIONLESS OIL FORMATION VOLUME FACTOR VS. DIMENSIONLESS PRESSURE FOR SATURATED CRUDES

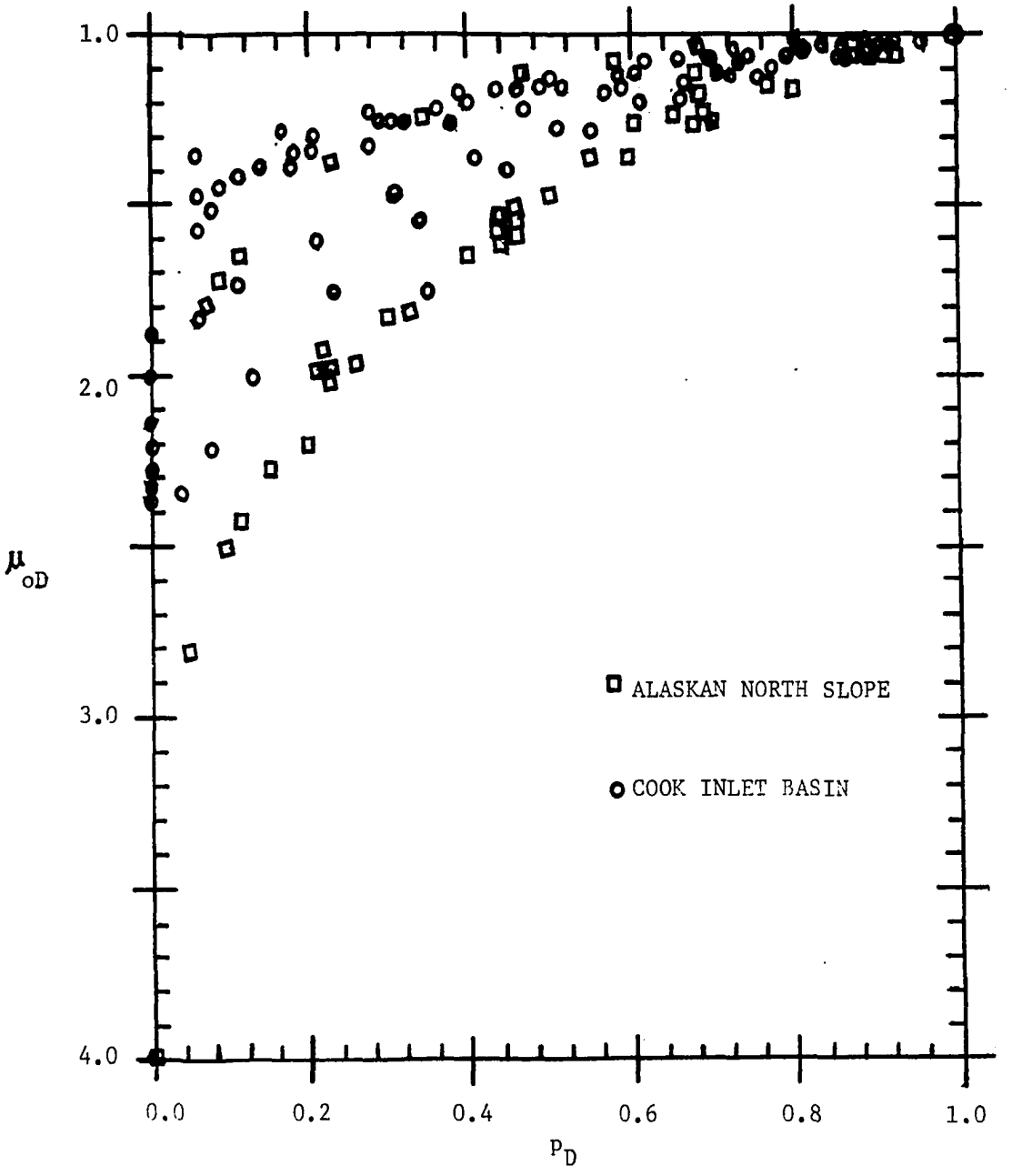

FIG. 25a : DIMENSIONLESS LIVE OIL VISCOSITY VS. DIMENSIONLESS PRESSURE FOR SATURATED CRUDES

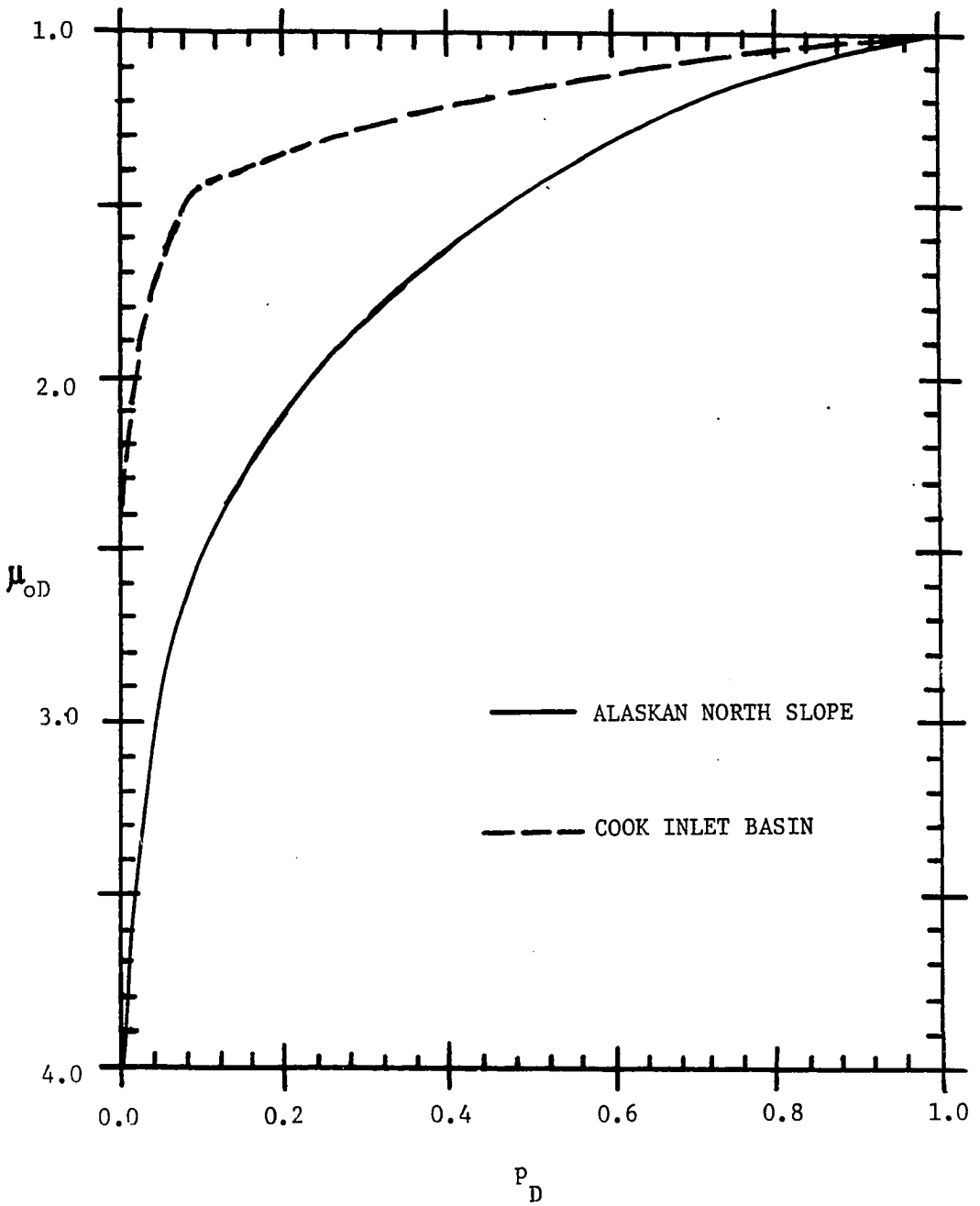

FIG. 25b : DIMENSIONLESS LIVE OIL VISCOSITY VS. DIMENSIONLESS PRESSURE FOR SATURATED CRUDES

CHAPTER VI

SUMMARY AND CONCLUSIONS

Alaskan crude oils are characterized by high non-hydrocarbon contents, like nitrogen and/or carbon dioxide, depending on the field. The presence of non-hydrocarbon contents in oils have significant effects on the prediction of the reservoir fluid properties. In this study, only the effect of nitrogen on bubble-point pressure, oil formation volume factor at bubble-point and live oil viscosity at bubble-point, of Cook Inlet Basin crude oils was investigated in great detail.

Predictions of reservoir fluid properties using the presently published correlations, showed that nitrogen correlation factors must be applied to get reasonable degree of accuracy. Additions to the predicted bubble-point pressure were noticed to increase as the temperature and methane content decrease. For the formation volume factor at bubble-point, the predicted values were also low and the nitrogen correction factors required were noticed to increase as the temperature and methane content increase. The required nitrogen content correction factors for live oil viscosity at bubble-point, were noticed to increase as the temperature increase and has an opposite effect with respect to methane content.

The discrepancies using the presently published PVT correlations, inspired the development of improved

prediction methods for some of the most commonly required oil reservoir properties of Alaskan fields. These prediction methods are in form of graphs or charts and equations, which are convenient to use with computers or calculators. Using these newly developed Alaskan crude oils PVT correlations, the following conclusions were reached:

1. Standard deviation of predicted bubble-point pressure from experimental values was 5.03 percent for CIB crude oils, and was 4.78 percent for ANS crude oils. With the published PVT correlations, the standard deviations ranged from 21.50 percent to 29.72 percent for CIB crude oils, and from 6.27 percent to 27.51 percent for ANS crude oils.

2. Standard deviation of predicted formation volume factor at bubble-point from experimental values was 0.199 percent for CIB crude oils, and was 0.789 percent for ANS crude oils. With the published PVT correlations, the standard deviations ranged from 1.138 percent to 4.344 percent for CIB crude oils, and from 0.951 percent to 1.852 percent for ANS crude oils.

3. Standard deviation of predicted live oil viscosity at bubble-point from experimental values was 4.21 percent for CIB crude oils, and was 16.14 percent for ANS crude oils. With the published PVT correlations, the standard deviations ranged from 10.09 percent to 12.08 percent for CIB crude oils, and from 31.16 percent to 33.35 percent for ANS crude oils.

Alaskan reservior fluid behaviors have also been developed into dimensionless correlations, in form of graphs and equations, to facilitate the analysis of depletion-drive oil reservoirs for which no laboratory PVT analysis is available. The predictions of solution gas-oil ratio, oil formation volume factor for saturated crude oils, and live oil viscosity for saturated crude oils, using the dimensionless correlations are within reasonable degree of accuracy.

REFERENCES

1. Beal, C. : "The Viscosity of Air, Water, Natural Gas, Crude Oil and Its Associated Gases at Oil Field Temperatures and Pressures", Trans., AIME (1946) 165, 94-115.
2. Beggs, H.D., and Robinson, J.R.: "Estimating the Viscosity of Crude Oil Systems", J. Pet. Tech. (Sept. 1975) 1140-1141.
3. Blasko, D.P., Wenger, W.J., and Dorris, J.C.: "Oilfields and Crude Oil Characteristics-Cook Inlet Basin, Alaska", U.S. Bu. Mines, RI 7688 (1972).
4. Borden, G., Jr., and Rzasa, M.J.: "Correlation of Bottom Hole Sample Data", Trans. AIME (1950) 189,345-348.
5. Cronquist, C.: "Dimensionless PVT Behavior of Gulf Coast Reservoir Oils", J. Pet. Tech. (May 1973) 538-542.
6. Davis, D.S.: "Empirical Equations and Nomography", McGraw-Hill Book Company, New York (1943).
7. Dodson, C.R., Goodwill, D. and Mayer, E.H.: "Application of Laboratory PVT Data to Reservoir Engineering Problems", Trans., AIME (1953) 198, 287-298.
8. Glaso, O. : "Generalized Pressure-Volume-Temperature Correlations", J. Pet. Tech. (May 1980) 785-795.

9. Jacobson, H.A.: "The Effect of Nitrogen on Reservoir Fluid Saturation Pressure", J. Can. Pet. Tech. (July-Sept. 1967) 101-105.

10. Jacoby, R.H., and Yarborough, L.: "PVT Measurements on Petroleum Reservoir Fluids and Their Uses", Ind. Eng. Chem. (Oct. 1967) 59, 49-61.

11. Katz, D.L.: "Prediction of the Shrinkage of Crude Oils", Drill and Prod. Prac., API (1942) 137-147.

12. Knopp, C.R., and Ramsey, L.A.: "Correlation of Oil Formation Volume Factor and Solution Gas-Oil Ratio", J. Pet. Tech. (Aug. 1960) 27-29.

13. Lasater, J.A. : "Bubble-Point Pressure Correlation", Trans., AIME (1958) 213,379-381.

14. Magoon, L.B., and Claypool, G.E.: "Two Oil Types on North Slope of Alaska-Implications for Explorations", AAPG Bullentin, v.65, No.4 (April 1981) 644-652.

15. McCain, W.D., Jr. : "The Properties of Petroleum Fluids", Pennwell Publ. Co., Tulsa, Oklahoma (1973).

16. Meehan, D.N. : "Improved Oil PVT Property Correlations", Oil & Gas J. (Oct. 27, 1980) 64-71.

17. Meehan, D.N. : "Crude Oil Viscosity Correlation", Oil & Gas J. (Nov.10, 1980) 214-216.

18. Ostermann, R.D., Ehlig-Econmides, C.A., and Owolabi, O.O. : "Correlations for the Reservoir Fluid Properties of Alaskan Crudes", paper SPE 11703 presented at the SPE 1983 California Regional Meeting, Ventura, California, March 23-25, 1983.

19. Standing, M.B. : "A Pressure-Volume-Temperature Correlation for Mixtures of California Oils and Gases", Drill. and Prod. Prac., API (1947) 275-287.

20. Standing, M.B. : "Volumetric and Phase Behavior of Oil Field Hydrocarbon Systems", Millet the Printer, Inc., Dallas (1977), 70-95.

21. Vazquez, M., and Beggs, H.D. : "Correlations for Fluid Physical Property Prediction", J. Pet. Tech. (June 1980) 968-970.

APPENDIX A

NOMENCLATURE

B_o = Oil formation volume factor, res.Bbl/STB.

B_{oa} = Oil formation volume factor at atmospheric pressure and reservoir temperature, res.Bbl/STB.

B_{ob} = Oil formation volume factor at the bubble-point pressure, res.Bbl/STB.

B^*_{ob} = Correlating number for calculating oil formation volume factor at the bubble-point pressure.

B_{od} = Differential oil formation volume factor, res.Bbl/Bbl.

B_{odb} = Differential oil formation volume factor at the bubble-point pressure, res.Bbl/Bbl.

B_{OD} = Dimensionless formation volume factor.

B_{of} = Flash oil formation volume factor, res.Bbl/STB.

B_{ofb} = Flash oil formation volume factor at the bubble-point pressure, res.Bbl/STB.

C = Bubble-point pressure correction factor for non-hydrocarbon gases.

C_1 = Methane

Co = Oil compressibility, vol./vol. - psi.

Co_2 = Carbon dioxide

f = Function

h = Function

N_2 = Nitrogen

P = Reservoir pressure, psia

P_b = Bubble-point pressure, psia

P_b^* = Correlating number for calculating bubble-point pressure.

P_D = Dimensionless reservoir pressure.

P_s = Separator pressure, psia

R_s = Solution gas-oil ratio, Scf/STB.

R_{sb} = Solution gas-oil ratio at the bubble-point, Scf/STB.

R_{sd} = Differential solution gas-oil ratio, Scf/Bbl.

R_{sD} = Dimensionless solution gas-oil ratio.

R_{sdb} = Differential solution gas-oil ratio at the bubble-point, Scf/Bbl.

R_{sf} = Flash solution gas-oil ratio, Scf/STB.

R_{sfb} = Flash solution gas-oil ratio at the bubble-point, Scf/STB.

T = Reservoir temperature, ^oF

T_s = Separator temperature, ^oF

Yg = Mole fraction of vapor phase of separator liquid.

γ_{API} = Stock tank oil gravity, ^{o}API

γ_{API}^* = Residual oil gravity, ^{o}API

γ_g = Average gas gravity of combined surface gases, (air=1)

γ_{gs} = Average gas gravity of combined surface gases corrected to a separator temperature and pressure of 60^{o}F and 100psig.

γ_o = Specific gravity of stock tank oil from flash separator, 60/60°F

γ_{st} = Specific gravity of stock tank oil, (water=1)

ρ_{st} = Effective molar density of stock tank oil, lb. mole/STB

μ_o = Live oil viscosity, cp

μ_{ob} = Live oil viscosity at the bubble-point pressure, cp

μ_{ob}^* = Correlating number of calculating live oil viscosity at the bubble-point pressure.

μ_{od} = Dead or gas-free oil viscosity, cp

μ_{oD} = Dimensionless live oil viscosity

μ_{odf} = Residual oil viscosity of a differential flash oil at reservoir temperature, cp

APPENDIX B

SI METRIC CONVERSION FACTORS

^{o}API		$141.5/(131.5 + {}^{o}API)$	=	g/cm^3
bbl	x	1.589 873 E-01	=	m^3
cp	x	1.0* E-03	=	Pa-s
cuft	x	2.831 685 E-02	=	m^3
ft	x	3.048* E-01	=	m
^{o}F		$({}^{o}F + 459.67)/1.8$	=	^{o}K
lb_m	x	4.535 924 E-01	=	Kg
ml	x	1.0* E+00	=	cm^3
psi	x	6.894 757 E+00	=	KPa

* Conversion factor is exact

APPENDIX C

PUBLISHED CORRELATING EQUATIONS

Bubble-Point Pressure

1. The correlation made by Standing[19], is given as:

$$P_b = 18.2\ [A\ (R_s/\gamma_g)\ ]^{0.83} - 1.4\ ] \qquad (C1)$$

where,

$$A = 10\ (^{0.00091T - 0.0125\gamma_{API}}) \qquad (C2)$$

2. Lasater's[13] correlation can be represented by the following equations:

$$P_b = P_f\ \frac{(T + 459.6)}{\gamma_g} \qquad (C3)$$

where,

$$\ln P_f = 2.303 + 2.5877U + 0.62102U^2 + 0.07037U^3 \qquad (C4)$$

with U = ln Yg.

Yg, the mole fraction of separator fluid in the vapor phase is calculated as:

$$\gamma_g = \frac{R_s/379.3}{R_s/379.3 + P_{st}} \qquad (C5)$$

P_{st} is the effective molar density of the stock tank oil in lb. mole/STB given by:

$$P_{st} = \frac{30.93\ \gamma_{st}^3}{\gamma_{st}^2 - 1.289\ \gamma_{st} - 0.4198} \qquad (C6)$$

Equation (C6) is based on Lasater's correlation for the effective molecular weight of the stock tank oil with respect to stock tank oil gravity.

3. The correlation of Vazquez and Beggs[21] uses separate correlating equations for crude oils with specific gravity above and below 30°API.

For $\gamma_{API} \leq$ 30 °API:

$$P_b = 20.788 \left\{\frac{R_s}{\gamma_{gs}}\right\}^{0.9143} \cdot \exp\left[\frac{-23.5202\ \gamma_{API}}{T + 460}\right] \qquad (C7)$$

For $\gamma_{API} >$ 30°API:

$$P_b = 29.782 \left\{\frac{R_s}{\gamma_{gs}}\right\}^{0.8425} \cdot \exp\left[\frac{-20.161\ \gamma_{API}}{T + 460}\right] \qquad (C8)$$

where,

$$\gamma_{gs} = \gamma_g \left[1 + 5.912 \times 10^{-5}\ \gamma_{API} \cdot T_s \cdot \log\left(P_s/114.7\right)\right] \qquad (C9)$$

4. The correlation of Glaso[8], is given by the following equations:

$$\log P_b = 1.7669 + 1.7447 \log P_b^* - 0.30128 (\log P_b^*)^2 \quad (C10)$$

where:

$$P_b^* = \left(\frac{R_s}{\gamma_g}\right)^{0.816} \cdot \left[\frac{T^{0.172}}{\gamma_{API,\ corr.}^{0.989}}\right] \quad (C11)$$

The Glaso's[8] correlation was based on North Sea crudes with a UOP paraffinicity factor of $K_{uop} = 11.9$. To allow the correlation to be used with crudes of different paraffinicity, a correction factor based on the viscosity and API gravity of the residual oil from a differential liberation, must be applied to the measured stock tank oil gravity. The corrected gravity is calculated by:

$$\gamma_{API,\ corr} = \left[\frac{\gamma^*_{API,\ corr}}{\gamma^*_{API}}\right] \cdot \gamma_{API} \quad (C12)$$

where,

$$\gamma^*_{API,\ corr} = 10^{(3.184 \times 10^{-11} \cdot T^{3.444} \cdot \mu_{odf})^B} \quad (C13)$$

with,

$$B = (10.213 \log T - 36.447)^{-1} \qquad (C14)$$

Correction Factors for Non-Hydrocarbon Contents

1. Glaso[8] reported the following equations for corrections in the bubble-point pressure when nitrogen, carbon dioxide, or hydrogen sulfide are present.

For nitrogen;

$$C_{N_2} = 1.0 + [-2.65\times10^{-4}\gamma_{API} + 5.5\times10^{-3}T + (0.0931\ \gamma_{API} - 0.8295)]\ Y_{N_2} + [1.954\times10^{-11}\ \gamma_{API}\ 4.699\ T + (0.027\ \gamma_{API} - 2.3666)]\ (Y_{N_2})^2 \qquad (C15)$$

For carbon dioxide;

$$C_{co_2} = 1.0 - 693.8\ Y_{co_2}\ T^{-1.553} \qquad (C16)$$

For hydrogen sulfide;

$$C_{H_2S} = 1.0 - (0.9035 + 0.00015\ \gamma_{API})\cdot Y_{H_2S} + 0.019\ (45 - \gamma_{API})\ (Y_{H_2S})^2 \qquad (C17)$$

2. Jacobson[9] reported the following correction for nitrogen content to be used with Standing's[19] correlation:

$$C_{N_2} = 15.85 + 286\ Y_{N_2} - 0.1077 \qquad (C18)$$

OIL FORMATION VOLUME FACTOR AT THE BUBBLE-POINT

1. Standing's[19] correlation is given by:

$$B_{ob} = 0.9759 + 12x10^{-5}\ [R_s\ \{\frac{\gamma_g}{\gamma_o}\}^{0.5} + 1.25\ T\ ]^{1.2} \qquad (C19)$$

2. The correlation of Glaso[8] is given by the following equations:

$$\log\ (B_{ob}{}^{-1}) = -6.588511+2.91329\ (\log\ B_{ob}^{*}) -0.27683\ (\log\ B_{ob}^{*})^2 \qquad (C20)$$

where,

$$B_{ob}^{*} = R_s\ \{\frac{\gamma_g}{\gamma_o}\}^{0.526} + 0.968\ T \qquad (C21)$$

3. The correlation of Vazquez and Beggs[21] is divided into two ranges dependent on the stock tank oil gravity.

For $\gamma_{API} \leq 30^{\circ}$ API:

$$Bob = 1.0 + 4.67 \times 10^{-4} R_s + 1.1 \times 10 (T-60) (\gamma_{API}/\gamma_{gs}) + 1.337 \times 10^{-9} R_s (T-60) (\gamma_{API}/\gamma_{gs}) \quad (C22)$$

For $\gamma_{API} > 30^{0}$ API,

$$Bob = 1.0 + 4.677 \times 10^{-4} Rs + 1.751 \times 10^{-5} (T-60) (\gamma_{API}/\gamma_{gs}) - 1.811 \times 10^{-8} R_s (T-60) (\gamma_{gs}/\gamma_{gs}) \quad (C23)$$

ALASKA OIL FIELDS / RESERVOIR DATA	BEAVER CREEK (C.I.B.)	GRANITE POINT (C.I.B.)	KATALLA (GULF OF ALASKA)	McARTHUR RIVER TRADING BAY UNIT (C.I.B.)			MIDDLE SHOAL	
PRODUCING FORMATION OIL ZONE	TYONEK	KENAI ZONE	KATALLA	HEMLOCK	TYONEK (MIDDLE KENAI G.)	WEST FORELAND	TYONEK "A" POOL	TYO ("B. C PO
DISCOVERY DATE	JAN. 14, 1973	JUNE 9, 1965	1902	OCT. 24, 1965			JUNE	
REFERENCE DATUM FEET BELOW SEA LEVEL	14,800	8,780		9,350	8,850	9,650	5,500	6,
ORIGINAL PRESSURE psia	7,552	4,251		4,250	4,009	4,457	2,508	2,
PRESSURE 12/31/80 psia	4,500	2,200		3,820	3,050	2,875	2,508	2,
SATURATION PRESSURE psia		2,400		1,787	1,826	1,186		1,
TEMPERATURE °F	215	135-170		180	163	185	128	1
OIL GRAVITY °API	35	41-44	41-45	35.4	35.6	32.9	42	3
ORIGINAL GAS/OIL RATIO SCF/STB	280	1,110		404	297	271	3,850	
GAS/OIL RATIO 12/31/80 SCF/STB				286	324	225		
FVF AT ORIGINAL PRESSURE RB/STB				1.25	1.23	1.19		
FVF AT SATURATION PRESSURE RB/STB				1.28	1.26	1.22		
OIL VISCOSITY AT ORIGINAL PRESSURE cp				1.190	1.088	1.497		
OIL VISCOSITY AT SATURATION PRESSURE cp				0.960	0.888	1.130		

ALASKA GAS FIELD / RESERVOIR DATA	ALBERT KALOA (C.I.B.)	BEAVER CREEK (C.I.B.)		BELUGA RIVER (C.I.B.)		BIRCH HILL (C.I.B.)
PRODUCING FORMATION GAS POOL	TYONEK	STERLING	BELUGA	STERLING	BELUGA	TYONEK
DISCOVERY DATE	JAN. 4, 1968	FEB. 10, 1967		DEC. 18, 1962		JUNE 9, 1965
REFERENCE DATUM FEET BELOW SEA LEVEL		5,000	8,100	3,300	4,500	7,960
ORIGINAL PRESSURE psia		2,200	3,800	1,635	2,215	3,840
PRESSURE 12/30/80 psia		2,200	3,800	1,490	1,710	
TEMPERATURE °F		107	142	94	106	136
GAS SPECIFIC GRAVITY		0.560		0.556	0.556	0.561

ALASKA GAS FIELD / RESERVOIR DATA	McARTHUR RIVER TRADING BAY UNIT (C.I.B.)		MOQUAWKIE (C.I.B.)		NICOLAI CREEK (C.I.B.)	NORTH COOK INLET (C.I.B.)	
PRODUCING FORMATION GAS POOL	TYONEK MIDDLE KENAI	UNDEFINED	TYONEK MIDDLE GROUND SHOAL MBR	CHUITNA MBR	BELUGA	STERLING	BELUGA
DISCOVERY DATE	DEC. 2, 1968		NOV. 28, 1965		MAY 1, 1966	SEPT. 1, 1962	
REFERENCE DATUM FEET BELOW SEA LEVEL						4,200	5,100
ORIGINAL PRESSURE psia	1,734		2,305	1,260	1,685	2,040	2,478
PRESSURE 12/30/80 psia						1,580	1,580
TEMPERATURE °F	117	110	108	80	110	109	119
GAS SPECIFIC GRAVITY	0.564		0.600		0.575	0.566	0.566

TABLE 1 - OIL AND GAS FIELDS IN ALASKA

McARTHUR RIVER TRADING BAY UNIT (C.I.B.)			MIDDLE GROUND SHOAL (C.I.B.)			UNNAMED (POINT THOMSON UNIT (A.N.S.)		PRUDHOE BAY PRUDHOE BAY UNIT (A.N.S.)			REDOUBT SHOAL (C.I.B.)	SWANSON RIVER (KENAI PENIN.)		
HEMLOCK	TYONEK (MIDDLE KENAI G.)	WEST FORELAND	TYONEK "A" POOL	TYONEK ("B, C, & D" POOLS)	TYONEK - HEMLOCK ("E, F, & G" POOLS)	CRETACEOUS (?) WELL #1	CRETACEOUS (?) WELL #2	KUPARUK RIVER	SADLE - ROCHIT (SAG R. & SHUBLIK)	LISBURNE	HEMLOCK	34-10	HEMLOCK CENTER	SCU
OCT. 24, 1965			JUNE 10, 1962			SEPT., 1977		JAN. 1, 1968			SEPT. 27, 1968	AUG. 24, 1957		
9,350	8,850	9,650	5,500	6,000	8,500	13,000	11,600	6,200	8,800			10,780	10,560	10,300
4,250	4,009	4,457	2,508	2,768	4,220	9,500	8,500	3,210	4,390			5,700	5,700	5,550
3,820	3,050	2,875	2,508	2,125	2,500			3,210	4,085			4,727	4,376	4,398
1,787	1,826	1,186		1,900	1,500			2,980	4,390			1,050	1,140	1,350
180	163	185	128	130	155	200	180	150	200			180	180	180
35.4	35.6	32.9	42	36-38	36-38	18.5	21	23	28	27	28.1	30	30	36.5
404	297	271	3,850	650	381	5,800	500	450	730		286	175	175	350
286	324	225												
1.25	1.23	1.19						1.22	1.40			1.173	1.235	1.295
1.28	1.26	1.22						1.224						
1.190	1.088	1.497						1.8-4.0	0.81					
0.960	0.888	1.130							0.81	0.98				

A RIVER I.B.)	BIRCH HILL (C.I.B.)	EAST UMIAT (A.N.S.)	FALLS CREEK (C.I.B.)	IVAN RIVER (C.I.B.)	KAVIK (A.N.S.)		KE (A.
BELUGA	TYONEK	NINULUK CHANDLER UPPER CRETACEOUS	TYONEK	TYONEK	SAG RIVER	SADLE - ROCHIT	SHU
8, 1962	JUNE 9, 1965	MARCH 28, 1963	JUNE 25, 1961	OCT. 8, 1956	NOV. 5, 1969		JUNE
4,500	7,960	1,929	7,045	7,800	3,500	3,500	
2,215	3,840	750	3,404	4,130	2,391	2,400	2
1,710				4,130			
106	136	50	132	128	114	127	
0.556	0.561	0.600	0.600	0.560	0.588	0.587	0

CREEK .B.)	NORTH COOK INLET (C.I.B.)		NORTH FORK (C.I.B.)	NORTH MIDDLE GROUND SHOAL (C.I.B.)	SOUTH BARROW (A.N.S.)		STERLING (C.I.B.)	SWANS (C
UGA	STERLING	BELUGA	TYONEK MIDDLE GROUND SHOAL MBR.	UPPER KENAI	JURASSIC SOUTH BARROW UNDEFINED	EAST BARROW	STERLING	STE "B, D,
, 1966	SEPT. 1, 1962		DEC. 20, 1965	NOV. 15, 1964	APRIL 15, 1949		AUG. 4, 1961	AUG.
	4,200	5,100	7,200		2,250	2,000	5,030	2, 7,
85	2,040	2,478	3,410	4,190	1,103	1,000	2,200	1, 4,
	1,580	1,580			750	1,000		
0	109	119	140	144	63	58	109	
75	0.566	0.566	0.562		0.56	0.57	0.569	0

LASKA

	SWANSON RIVER (KENAI PENIN.)			TRADING BAY (C.I.B.)				UMIAT (A.N.S.)	UNNAMED FLAXMAN ISLAND AREA (A.N.S.)	UNNAMED KUPARUK RIVER S.S. "UGNU" RIVER AREA (A.N.S.)
	34-10	HEMLOCK CENTER	SCU	TYONEK (MIDDLE KENAI) "C"	"D"	HEMLOCK	TYONEK-HEMLOCK	CRETACEOUS	TERTIARY (?)	KUPARUK RIVER S.S.
	AUG. 24, 1957			JUNE 1, 1965				DEC. 26, 1946	SEPT. 11, 1975	APRIL 7, 1969
	10,780	10,560	10,300	4,000	5,628	6,100	9,800		12,500	7,000
	5,700	5,700	5,550	2,037	2,637	2,802	4,470		9,850	3,360
	4,727	4,376	4,398	2,140	1,880	1,960	4,150			
	1,050	1,140	1,350		1,921	1,622	1,780			
	180	180	180		112	136	180		195	150
	30	30	36.5	28	28	31.1	35.8 -36.2		23.1	22.9- 29.0
	175	175	350		268	318	275		864-934	228-413
	1.173	1.235	1.295				1.29			1.22
							1.036			

KAVIK (A.N.S.)		KEMIK (A.N.S.)	KENAI (C.I.B.)							LEWIS RIVER (C.I.B.)
RIVER	SADLE - ROCHIT	SHUBLIK	KENAI - STERLING					BELUGA	KENAI - TYONEK	BELUGA SAND
NOV. 5, 1969		JUNE 17, 1972	OCTOBER 11, 1969							OCT. 1, 1975
00	3,500		3,700	3,960	4,025	4,125	4,565	4,992	9,000	4,700
91	2,400	2,678	1,862	1,919	1,981	2,078	2,505	2,558	4,416	2,344
			1,268	1,267	1,302	1,327	1,350	1,645	1,646	
14	127	123	103	105	105	106	109	115	143	111
88	0.587	0.600	0.557	0.557	0.557	0.557	0.557	0.555	0.560	

STERLING (C.I.B.)	SWANSON RIVER (C.I.B.)	TRADING BAY (C.I.B.)	WEST FORELAND (C.I.B.)	WEST FORK (C.I.B.)
STERLING	STERLING "B, D, E" SANDS	TYONEK	TYONEK	STERLING
AUG. 4, 1961	AUG. 24, 1957	OCT. 5, 1979	MARCH 29, 1962	SEPT. 26, 1960
5,030	2,870- 7,500			
2,200	1,335- 4,500		4,265	2,037
				1,999
109	123		171	110
0.569	0.600	0.582	0.600	0.560